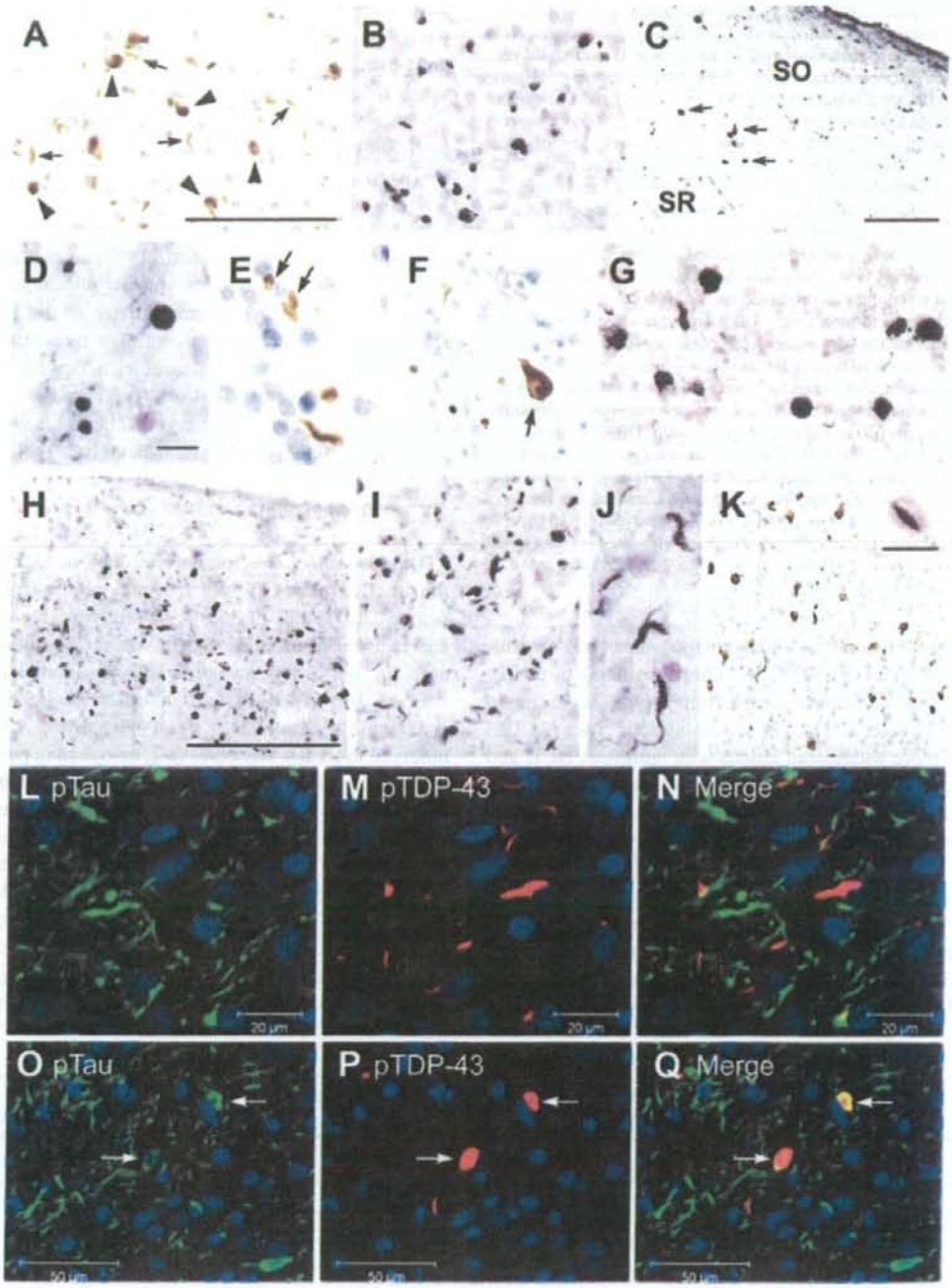

matter, including the stratum radiatum and the stratum oriens of the CA2/3 region, alveus and parahippocampal white matter. In double labeling immunofluorescence experiments, cortical tau-positive neuropil threads and TDP-43-positive dystrophic neurites were usually stained independently (Fig. 1l–n), while some neurons showed cytoplasmic inclusions immunoreactive for both markers (Fig. 1o–q).

In 19 cases with pTDP-43 immunoreactivity in the first series (Table 3), pTDP-43 pathology was largely restricted

◀ **Fig. 1** Phosphorylated TDP-43 (*pTDP-43*) positive structures in Alzheimer's disease cases with diffuse type of TDP-43 pathology. **a** Neuronal cytoplasmic inclusions (NCIs) (*arrowheads*) and dystrophic neurites (DNs) (*arrows*) in amygdala. **b** NCIs in the granule cells of the dentate gyrus. **c** NCIs in the principal layer (*arrows*) and small round or short threads-like structures in the stratum oriens (*SO*) and stratum radiatum (*SR*) of the CA2/3 region. **d** A high power view of small round or short threads-like structures in the stratum oriens of the CA2/3 region. **e** Glial cytoplasmic inclusions (*arrows*) and a small round or a short threads-like structure in the alveus of the CA1 region. **f** A neurofibrillary tangle-like structure (*arrow*), small round structures and short neurites in the principal layer of the CA1 region. **g** Large NCIs and short neurites in the subiculum. **h** Massive NCIs and DNs in the superficial layer of the entorhinal cortex. **i** A high power view of NCIs and DNs in the entorhinal cortex. **j** Glial cytoplasmic inclusions in the white matter of the parahippocampal gyrus. **k** Numerous NCIs and DNs in the superficial layer of the lateral occipitotemporal cortex. *Inset* shows a neuronal intranuclear inclusion with a lentiform shape. Double label immunofluorescence (**l–q**) demonstrates that most tau-positive neuropil threads (*green fluorescence* in **l**) and pTDP-43 positive DNs (*red fluorescence* in **m**) in the temporal neocortex are independent (**n**), while there is partial colocalization of tau and pTDP-43 in some neuronal cytoplasmic inclusions (*arrows* in **o–q**). Immunohistochemistry using primary antibodies pS403/404 (**a, e, f, k**) and pS409/410 (**b, c, d, g, h, i, j**). Double label immunofluorescence with anti-phosphorylated tau (AT8) and pS403/404 (**l–q**). *Scale bars* **a, b, c, f, g, i** 100 μm; **d, e, j**, *inset* in **k** 10 μm; **h, k** 200 μm

to the limbic region (amygdala, hippocampus and entorhinal cortex) in 14 cases (73.7%). This distribution of pTDP-43 pathology corresponds to the "limbic type" according to Amador-Ortiz et al. [1]. The remaining four cases (21.1%) showed more widespread lesions with numerous NCIs and DNs in the temporal neocortex; corresponding to the "diffuse type" according to Amador-Ortiz et al. [1]. Of the 14 cases with pTDP-43 immunoreactivity in the second series (Table 4), pTDP-43 pathology was found only in the amygdala in 4 cases (28.6%), showed more widespread involvement of limbic structures in 5 cases (35.7%) and extended into the cerebral neocortex in the remaining 5 cases (35.7%).There appeared to be a hierarchy to the anatomical distribution and severity of involvement that was best demonstrated in the second series (Table 4). The pathology seemed to start in the amygdala and then progress to other limbic structures before involving the neocortex. Among neocortical regions, the temporal lobe was always involved, the frontal lobe less frequently and only rarely the parietal lobe was affected.

The mean age at death was significantly higher in cases with pTDP-43 immunoreactivity in the second series ($P = 0.015$). A similar tendency was also observed in the first series, but it was not statistically significant ($P = 0.16$). The Braak NFT stage score was significantly higher in cases with pTDP-43 immunoreactivity in the first series ($P = 0.027$). This correlation could not be assessed in the second series since there was insufficient range in the Braak stage among the cases (Tables 1, 4). There were no differences in sex or brain weight between the cases with pTDP-43 immunoreactivity and those without (see Table 1).

Accumulation of phosphorylated TDP-43 in DLB

pTDP-43-positive structures were found in 53% (7/15) of the first DLB series (Tables 1, 5) and in 60% (6/10) of the second DLB series (Tables 1, 6) with variable frequency and regional distribution. There was no significant difference in the frequency of pTDP-43 immunoreactivity between the two series ($\chi^2 = 0.000$; 1 *df*; $P > 0.999$).

Figure 2 illustrates pTDP-43-positive structures observed in DLB + AD cases (a–j, m–o) and in pure DLBD cases (k, l). The morphology and anatomical distribution of the pathology was similar to that seen in the series of AD cases and the neocortical involvement again resembled FTLD-U Type 3 with a few lentiform NIIs. In double labeling confocal microscopy for pTDP-43 and phosphorylated α-synuclein in the cortex, some neurons showed cytoplasmic inclusions immunoreactive for both markers (m–o).

Of the eight cases with pTDP-43 immunoreactivity in the first DLB series (Table 5), TDP-43 pathology was

Table 5 TDP-43-positive structures in the first series of dementia with Lewy bodies

Case no.	Age	Sex	SP (CERAD)	NFT (Braak)	DLB likelihood	Pathological diagnosis	Amyg	DG	CA4	CA2/3	CA1	Sub	EC	Temp	TDP-43 path
F-DLB1	63	F	C	VI	Int.	DLB + AD	NA	+++	+	++	+	++	+++	++	Diffuse
F-DLB2	67	M	C	VI	Int.	DLB + AD	+++	+++	+	++	+	++	+++	++	Diffuse
F-DLB3	82	F	C	VI	Int.	DLB + AD	NA	+	±	+	+	++	++	+	Diffuse
F-DLB4	83	M	C	IV	High	DLB + AD	+++	+	−	+	+	++	+++	−	Limbic
F-DLB5	89	M	C	IV	High	DLB + AD	NA	−	−	+	−	+	+	−	Limbic
F-DLB6	71	M	C	IV	High	DLB + AD	NA	±	−	±	−	±	±	−	Limbic
F-DLB7	51	M	0	II	High	DLB	++	+	+	++	±	++	++	−	Limbic
F-DLB8	82	M	0	II	High	DLB	+	−	−	−	−	−	+	−	Limbic

SP Senile plaque, *NFT* neurofibrillary tangle, *Amyg* amygdala, *DG* dentate gyrus, *Sub* subiculum, *EC* entorhinal cortex, *Temp* temporal cortex, *path* pathology, *NA* not available

−, None; ±, slight; +, mild; ++, moderate; +++, severe

Table 6 TDP-43-positive structures in the second series of dementia with Lewy bodies

Case no.	Age	Sex	SP (CERAD)	NFT (Braak)	DLB likelihood	Pathological diagnosis	Amyg	DG	CA4	CA2/3	CA1	Sub	EC	Cing	Temp	Front	Par	TDP-43 path
S-DLB1	90	F	C	VI	Int.	DLB + AD	+++	–	–	–	–	+	±	–	–	–	–	Limbic
S-DLB2	79	M	C	VI	Int.	DLB + AD	++	–	–	–	–	–	±	–	–	–	–	Limbic
S-DLB3	74	M	0	II	High	DLB	+	–	–	–	–	–	–	–	–	–	–	Amygdala
S-DLB4	70	M	C	II	High	DLB	+	NA	NA	NA	NA	NA	NA	–	–	–	–	Amygdala
S-DLB5	71	M	C	III	High	DLB	±	–	–	–	–	–	–	–	–	–	–	Amygdala
S-DLB6	74	F	C	VI	Int.	DLB + AD	±	–	–	–	–	–	–	–	–	–	–	Amygdala

SP Senile plaque, *NFT* neurofibrillary tangle, *Amyg* amygdala, *DG* dentate gyrus, *Sub* subiculum, *EC* entorhinal cortex, *Cing* cingulate cortex, *Temp* temporal cortex, *Front* frontal cortex, *Par* parietal cortex, *path* pathology, *NA* not available

–, None; ±, slight; +, mild; ++, moderate; +++, severe

largely confined to limbic region in five cases (62.5%), while three cases (37.5%) revealed more widespread lesions in the temporal cortex. In the second series (Table 6), four cases (66.7%) showed slight TDP-43 pathology only in amygdala and the remaining two cases (33.3%) showed moderate to severe TDP-43 pathology in amygdala and slight to mild TDP-43 pathology in limbic region.

There were no significant differences in the mean age at death, sex and Braak NFT stage score between cases with pTDP-43 immunoreactivity and those without, in either series (see Table 1). All three cases with pure DLB had some TDP-43 pathology.

Biochemical analyses of accumulated TDP-43 in AD and DLB

Figure 3 shows immunoblot analyses of sarkosyl-insoluble, urea-soluble fractions extracted from brains of a normal control (lane 1), AD without pTDP-43 immunoreactivity (AD−, lane 2), DLB with pTDP-43 immunoreactivity (DLB+, F-DLB2, see Table 5) (lane 3), AD with pDP-43 immunoreactivity (AD+, F-AD1, see Table 3) (lane 4), FTLD-U, Type 3 (lane 5), and FTLD-U, Type 1 (lane 6). With phosphorylation-dependent antibodies specific for pS409/410 (a) and for pS403/404 (b), intense immunoreactivity throughout the gel was observed only in DLB+ (lane 3), AD+ (lane 4), FTLD-U, Type 3 (lane 5), and FTLD-U, Type 1 (lane 6). Regarding low-molecular-weight fragments, DLB+ (lane 3) and AD+ (lane 4) showed a similar pattern with three major bands at 23, 24 and 26 kDa and two minor bands at 18 and 19 kDa. Of three major bands, a 23 kDa band was the most intense, while the immunoreactivity of two minor bands at 18 and 19 kDa was similar. This band pattern corresponds to that of FTLD-U, Type 3 (see lane 5 in a, b and schematic diagram in c), previously reported by us [14]. FTLD-U with Type 1 (lane 6) showed a band pattern with two major bands at 23 and 24 kDa and two minor bands at 18 and 19 kDa, which is consistent with our previous report [14].

Discussion

In this study, we used phosphorylation-dependent anti-TDP-43 antibodies to perform detailed immunohistochemical and biochemical examination of two independent series of brains with AD and DLB. We found higher frequencies of TDP-43 pathology in AD (36–56%) and DLB (53–60%) than in previous reports [1, 16, 17, 19, 28, 36]. This may be due to the two immunohistochemical protocols we employed, one on free-floating sections and the other using an automated immunostainer for paraffin sections, are more sensitive than the methods used in previous studies. In addition, the higher frequencies found in our second series are partially explained by inclusion of examination of the amygdala, the region that appears to be most often affected by TDP-43 pathology [17].

The largely consistent observations between our two series, despite differences in the ethnic populations and source of the clinical cases, suggest that our findings are more likely to be broadly applicable to other populations of AD and DLB patients. We have also demonstrated that similar findings are attainable using various immunohistochemical methodology employed by different labs.

In immunohistochemical examinations of AD and DLB cases in the present study, phosphorylation-dependent anti-TDP-43 antibodies stained NCIs and DNs in the cerebral grey matter as previously reported [1, 16, 30, 39], and some thread-like or coiled body-like structures in the whiter matter. Regarding the distribution of TDP-43 pathology in AD, Amador-Ortiz et al. [1] first classified it into limbic and diffuse types, and indicated that limbic involvement was more common. Subsequently, Hu et al. [17] found some AD cases with TDP-43 pathology confined to the amygdala only. They suggested that the amygdala is the most susceptible

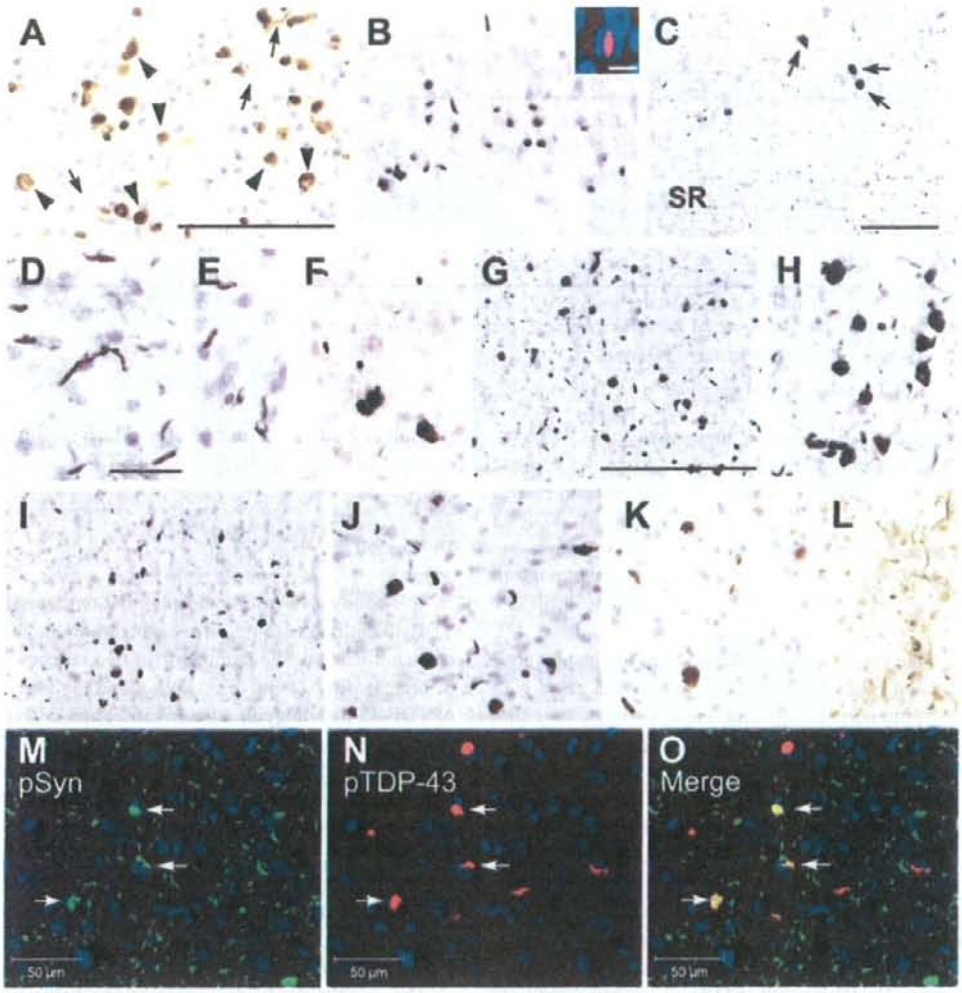

Fig. 2 Phosphorylated TDP-43 (*pTDP-43*) positive structures in cases of dementia with Lewy bodies. TDP-43 positive structures in cases of DLB plus AD with diffuse type of TDP-43 pathology are shown in **a**–**j**. Neuronal cytoplasmic inclusions (NCIs) and dystrophic neurites (DNs) in the entorhinal cortex of the pure DLB cases without AD pathology are shown in **k** (F-DLB7) and **l** (F-DLB8). **a** NCIs (*arrowheads*) and DNs (*arrows*) in amygdala. **b** NCIs in the dentate granule cells. *Inset* shows immunofluorescence staining of a lentiform inclusion (*red*) in the nucleus (*blue*) of a granule cell. **c** NCIs in the principal layer (*arrows*) and massive short threads-like structures in the stratum radiatum (*SR*) of the CA2/3 region. **d** A high power view of short threads-like structures in the stratum radiatum of the CA2/3 region. **e** Short threads-like structure in the alveus of the CA1 region. **f** Large NCIs and short neurites in the subiculum. **g** Massive NCIs and DNs in the superficial layer of the entorhinal cortex. **h** A high power view of NCIs and DNs in the entorhinal cortex. **i** Numerous NCIs and DNs in the superficial layer of the lateral occipitotemporal cortex. **j** A high power view of NCIs and DNs in the lateral occipitotemporal cortex. Double label immunofluorescence (**m**–**o**) shows partial co-localization of α-synuclein and pTDP-43 in the NCIs in the temporal neocortex (*arrows*), whereas most α-synuclein-positive neurites are negative for pTDP-43 (**m**–**o**). Immunostaining with pS403/404 (**a**, **i**, **j**) and pS409/410 (**b**–**h**, **k**, **l**). Double label immunofluorescence with anti-phosphorylated α-synuclein (pα#64) and pS403/404 (**m**–**o**). *Scale bars* **a**, **b**, **f**, **h**, **j**–**l** 100 µm; **d**, **e** 25 µm; **c**, **g**, **i** 200 µm; *inset* in **b** 10 µm

region, and that TDP-43 pathology in AD spreads from limbic structures to association cortices. In the present study, we observed amygdala only, limbic, and diffuse patterns of pTDP-43 pathology, not only in AD cases but also in DLB cases. These results suggest a common progressive anatomical pattern of pTDP-43 pathology in AD and DLB, with sequential spread from the amygdala to other limbic structures and then to association cortices. Although the number of cases was small, the results from our second series also suggests that there may be hierarchical involvement

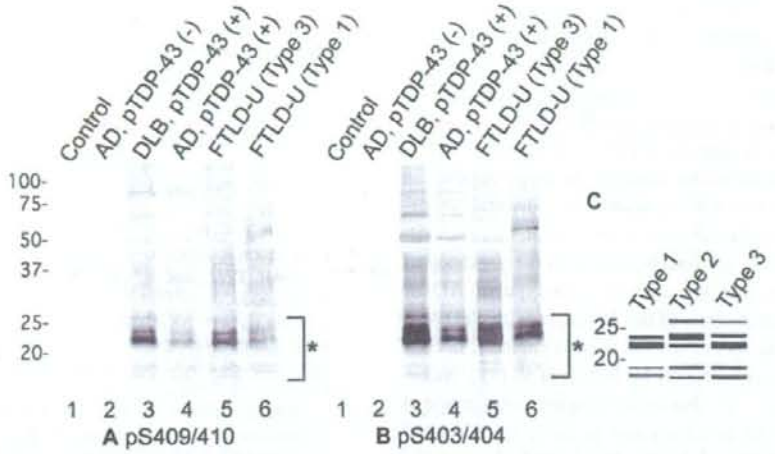

Fig. 3 The band pattern of the C-terminal fragments of phosphorylated TDP-43 (*pTDP-43*) in Alzheimer's disease (*AD*) and dementia with Lewy bodies (*DLB*). Immunoblot analyses of sarkosyl-insoluble, urea-soluble fractions, using phosphorylation-dependent anti-TDP-43 antibodies pS409/410 (**a**) and pS403/404 (**b**). *Lane 1* normal control; *lane 2* AD without pTDP-43 immunoreactivity (AD−); *lane 3* DLB with pTDP-43 immunoreactivity (DLB+); *lane 4* AD with pTDP-43 immunoreactivity (AD+); *lane 5* FTLD-U with Type 3 TDP-43 pathology; *lane 6* FTLD-U with Type 1 TDP-43 pathology. Schematic diagram (**c**) showing the band pattern of the C-terminal fragments of phosphorylated TDP-43 we have previously reported [14]. Strong immunoreactivity throughout the gel is observed only in DLB+ (*lane 3*), AD+ (*lane 4*) and FTLD-U (*lanes 5, 6*). DLB+ (*lane 3*), AD+ (*lane 4*) and FTLD-U, Type 3 (*lane 5*) show similar patterns of low M_r bands with three major bands at 23, 24 and 26 kDa and two minor bands at 18 and 19 kDa, while FTLD-U, Type 1 (*lane 6*) shows two major bands at 23 and 24 kDa and two minor bands at 18 and 19 kDa (*asterisk*)

of neocortical regions, with the temporal association cortex involved first, followed by the frontal lobe and parietal lobe last.

Since subclassification of FTLD-U is based on TDP-43 pathology in the neocortex [7, 25, 35], only AD and DLB cases with the diffuse type of TDP-43 pathology could be subtyped. All of these cases had pTDP-43-positive NCIs and short DNs in the upper cortical layers, which corresponds to FTLD-U Type 3. In addition, most of them (8 of 9 AD cases and 2 of 3 DLB cases with the diffuse type) also had a few pTDP-43-positive NIIs in the dentate gyrus or the neocortex, These findings are consistent with the previous reports by Uryu et al. [39] and Nakashima-Yasuda et al. [30], but differ somewhat from Joseph et al. [19] who reported all three FTLD-U subtypes in AD, with the majority being Type 2.

Perhaps the greatest significance of this study is the evidence it provides that the pathological TDP-43 that accumulates in AD and DLB is similar to that in FTLD-U. First, positive staining of abnormal structures in immunohistochemistry and of abnormal bands on immunoblots of sarkosyl-insoluble fraction with pS403/404 and pS409/410 antibodies suggest that C-terminal phosphorylation sites of TDP-43 accumulated in AD and DLB brains are common to those in FTLD-U brains [14]. Second, intense staining of low-molecular-weight bands around 20–25 kDa on immunoblotting of sarkosyl-insoluble fraction from AD and DLB cases with neocortical pTDP-43 pathology indicates that the generation of C-terminal fragments of TDP-43 takes place in brains of these diseases as it does in FTLD-U [14, 18]. Furthermore, the band pattern of C-terminal fragments in AD and DLB corresponds to that of FTLD-U, Type 3, found in our previous report [14]. These findings suggest that there may be a common process that leads to the accumulation of pathological TDP-43 in FTLD-U Type 3, and some cases of AD and DLB. In this context, it should be noted that cases of familial FTLD-U with *PGRN* mutations always show Type 3 TDP-43 pathology [7]. Some familial FTLD-U cases with *PGRN* mutations have additional AD pathology [29] or tau and α-synuclein pathology [22]. Several mutations and polymorphisms of *PGRN* have recently been identified in AD and Parkinson's disease populations [5, 6] and these might underlie the co-occurrence of abnormal deposition of TDP-43, tau, and α-synuclein. Furthermore, a common genetic variant in *PGRN* (rs5848), located within a binding site for miR-659, has recently been identified as a major susceptibility factor for sporadic FTLD-U [34]. Homozygosity for the T-allele of rs5848 causes a significant reduction in the level of PGRN protein and is associated with a 3.2-fold increased risk of developing FTLD-U. The majority of these cases have Type 3 TDP-43 pathology. It is therefore possible that the subset of AD and DLB patients who develop TDP-43 pathology are carriers of this, or some other genetic risk factor, for TDP-43 proteinopathy. Partial colocalization of tau and TDP-43 or α-synuclein and TDP-43 in some cytoplasmic inclusions found in this

and other studies [1, 11, 13, 16, 30] may argue against a direct interaction between these proteins, and support the notion that there may be genetic or environmental factors that make the subset of neurons vulnerable for intracellular accumulation of tau, α-synuclein and TDP-43.

The fact that the accumulated TDP-43 in AD and DLB is biochemically similar to that believed to be pathogenic in FTLD-U, suggests that it might contribute to neurodegeneration or modify the clinical course. At present, there is a little data regarding the relationship between the presence of TDP-43 pathology and the clinical phenotype of AD or DLB. The older age at death of the AD cases with pTDP-43 pathology, observed in our second series (Table 4), is consistent with the previous report by Joseph et al. [19]. Nakashima-Yasuda et al. [30] also found a higher average age at death in the TDP-43 positive cases in Lewy body related diseases with dementia. A higher Braak NFT stage in the TDP-43 positive patients was found in DLB + AD cases by Nakashima-Yasuda et al. [30] and also in our first series of AD (Table 1). Further studies using larger cohorts with more detailed clinical, radiological and pathological data are needed to elucidate the clinical impact of TDP-43 pathology in AD and DLB.

Acknowledgments We thank Ms. H. Kondo, Ms. Y. Izumiyama, Ms. C. Haga and Ms. M. Luk for their excellent technical assistance. This research was supported by a Grant-in-Aid for Scientific Research (C) (to TA), a Grant-in-Aid for Scientific Research on Priority Areas—Research on Pathomechanisms of Brain Disorders (to MH), a Grant-in-Aid for Scientific Research (B) (to MH) from the Ministry of Education, Culture, Sports, Science and Technology of Japan, a grant from the Canadian Institutes of Health Research (grant # 74580) (to IM) and a grant from the Pacific Alzheimer Research Foundation (to IM).

References

1. Amador-Ortiz C, Lin WL, Ahmed Z et al (2007) TDP-43 immunoreactivity in hippocampal sclerosis and Alzheimer's disease. Ann Neurol 61:435–445. doi:10.1002/ana.21154
2. Arai T, Hasegawa M, Akiyama H et al (2006) TDP-43 is a component of ubiquitin-positive tau-negative inclusions in frontotemporal lobar degeneration and amyotrophic lateral sclerosis. Biochem Biophys Res Commun 351:602–611. doi:10.1016/j.bbrc.2006.10.093
3. Arai T, Ikeda K, Akiyama H et al (2003) Different immunoreactivities of the microtubule-binding region of tau and its molecular basis in brains from patients with Alzheimer's disease, Pick's disease, progressive supranuclear palsy and corticobasal degeneration. Acta Neuropathol 105:489–498
4. Baker M, Mackenzie IR, Pickering-Brown SM et al (2006) Mutations in progranulin cause tau-negative frontotemporal dementia linked to chromosome 17. Nature 442:916–919. doi:10.1038/nature05016
5. Brouwers N, Nuytemans K, van der Zee J et al (2007) Alzheimer and Parkinson diagnoses in progranulin null mutation carriers in an extended founder family. Arch Neurol 64:1436–1446. doi:10.1001/archneur.64.10.1436
6. Brouwers N, Sleegers K, Engelborghs S et al (2008) Genetic variability in progranulin contributes to risk for clinically diagnosed Alzheimer disease. Neurology 71:656–664. doi:10.1212/01.wnl.0000319688.89790.7a
7. Cairns NJ, Neumann M, Bigio EH et al (2007) TDP-43 in familial and sporadic frontotemporal lobar degeneration with ubiquitin inclusions. Am J Pathol 171:227–240. doi:10.2353/ajpath.2007.070182
8. Cruts M, Gijselinck I, van der Zee J et al (2006) Null mutations in progranulin cause ubiquitin-positive frontotemporal dementia linked to chromosome 17q21. Nature 442:920–924. doi:10.1038/nature05017
9. Davidson Y, Kelley T, Mackenzie IRA et al (2007) Ubiquitinated pathological lesions in frontotemporal lobar degeneration contain the TAR DNA-binding protein, TDP-43. Acta Neuropathol 113:521–533. doi:10.1007/s00401-006-0189-y
10. Feldman H, Levy AR, Hsiung GY et al (2003) A Canadian cohort study of cognitive impairment and related dementias (ACCORD): study methods and baseline results. Neuroepidemiology 22:265–274. doi:10.1159/000071189
11. Freeman SH, Spires-Jones T, Hyman BT, Growdon JH, Frosch MP (2008) TAR-DNA binding protein 43 in Pick disease. J Neuropathol Exp Neurol 67:62–67. doi:10.1097/nen.0b013e3181609361
12. Gitcho MA, Baloh RH, Chakraverty S et al (2008) TDP-43 A315T mutation in familial motor neuron disease. Ann Neurol 63:535–538. doi:10.1002/ana.21344
13. Hasegawa M, Arai T, Akiyama H et al (2007) TDP-43 is deposited in the Guam parkinsonism–dementia complex brains. Brain 130:1386–1394. doi:10.1093/brain/awm065
14. Hasegawa M, Arai T, Nonaka T et al (2008) Phosphorylated TDP-43 in frontotemporal lobar degeneration and amyotrophic lateral sclerosis. Ann Neurol 64:60–70. doi:10.1002/ana.21425
15. Higashi S, Iseki E, Yamamoto R et al (2007) Appearance pattern of TDP-43 in Japanese frontotemporal lobar degeneration with ubiquitin-positive inclusions. Neurosci Lett 419:213–218. doi:10.1016/j.neulet.2007.04.051
16. Higashi S, Iseki E, Yamamoto R et al (2007) Concurrence of TDP-43, tau and alpha-synuclein pathology in brains of Alzheimer's disease and dementia with Lewy bodies. Brain Res 1184:284–294. doi:10.1016/j.brainres.2007.09.048
17. Hu WT, Josephs KA, Knopman DS et al (2008) Temporal lobar predominance of TDP-43 neuronal cytoplasmic inclusions in Alzheimer disease. Acta Neuropathol 116:215–220. doi:10.1007/s00401-008-0400-4
18. Igaz LM, Kwong LK, Xu Y et al (2008) Enrichment of C-terminal fragments in TAR DNA-binding protein-43 cytoplasmic inclusions in brain but not in spinal cord of frontotemporal lobar degeneration and amyotrophic lateral sclerosis. Am J Pathol 173:182–194. doi:10.2353/ajpath.2008.080003
19. Josephs KA, Whitwell JL, Knopman DS et al (2008) Abnormal TDP-43 immunoreactivity in AD modifies clinicopathologic and radiologic phenotype. Neurology 70:1850–1857. doi:10.1212/01.wnl.0000304041.09418.b1
20. Kabashi E, Valdmanis PN, Dion P et al (2008) TARDBP mutations in individuals with sporadic and familial amyotrophic lateral sclerosis. Nat Genet 40:572–574. doi:10.1038/ng.132
21. Kosaka K (1990) Diffuse Lewy body disease in Japan. J Neurol 237:197–204. doi:10.1007/BF00314594
22. Leverenz JB, Yu CE, Montine TJ et al (2007) A novel progranulin mutation associated with variable clinical presentation and tau, TDP43 and alpha-synuclein pathology. Brain 130:1360–1374. doi:10.1093/brain/awm069
23. Lin WL, Dickson DW (2008) Ultrastructural localization of TDP-43 in filamentous neuronal inclusions in various neurodegenerative diseases. Acta Neuropathol 116:205–213. doi:10.1007/s00401-008-0408-9
24. Mackenzie IR, Bigio EH, Ince PG et al (2007) Pathological TDP-43 distinguishes sporadic amyotrophic lateral sclerosis from

amyotrophic lateral sclerosis with SOD1 mutations. Ann Neurol 61:427–434. doi:10.1002/ana.21147
25. Mackenzie IRA, Baborie A, Pickering-Brown S et al (2006) Heterogeneity of ubiquitin pathology in frontotemporal lobar degeneration: classification and relation to clinical phenotype. Acta Neuropathol 112:539–549. doi:10.1007/s00401-006-0138-9
26. Mackenzie IRA, Baker M, Pickering-Brown S et al (2006) The neuropathology of frontotemporal lobar degeneration caused by mutations in the progranulin gene. Brain 129:3081–3090. doi:10.1093/brain/awl271
27. McKeith IG, Dickson DW, Lowe J et al (2005) Diagnosis and management of dementia with Lewy bodies: third report of the DLB Consortium. Neurology 65:1863–1872. doi:10.1212/01.wnl.0000187889.17253.b1
28. Morita M, Al-Chalabi A, Anderson PM et al (2006) A locus on chromosome 9p confers susceptibility to ALS and frontotemporal dementia. Neurology 66:839–844. doi:10.1212/01.wnl.0000200048.53766.b4
29. Mukherjee O, Pastor P, Cairns NJ et al (2006) HDDD2 is a familial frontotemporal lobar degeneration with ubiquitin-positive tau-negative inclusions caused by a missense mutation in the signal peptide of progranulin. Ann Neurol 60:314–322. doi:10.1002/ana.20963
30. Nakashima-Yasuda H, Uryu K, Robinson J et al (2007) Co-morbidity of TDP-43 proteinopathy in Lewy body related diseases. Acta Neuropathol 114:221–229. doi:10.1007/s00401-007-0261-2
31. Neumann M, Kwong LK, Sampathu DM, Trojanowski JQ, Lee VM (2007) TDP-43 proteinopathy in frontotemporal lobar degeneration and amyotrophic lateral sclerosis: protein misfolding diseases without amyloidosis. Arch Neurol 64:1388–1394. doi:10.1001/archneur.64.10.1388
32. Neumann M, Sampathu DM, Kwong LK et al (2006) Ubiquitinated TDP-43 in frontotemporal lobar degeneration and amyotrophic lateral sclerosis. Science 314:130–133. doi:10.1126/science.1134108
33. Newell KL, Hyman BT, Growdon JH, Hedley-Whyte ET (1999) Application of the National Institute on Aging (NIA)–Reagan Institute criteria for the neuropathological diagnosis of Alzheimer disease. J Neuropathol Exp Neurol 58:1147–1155. doi:10.1097/00005072-199911000-00004
34. Rademakers R, Eriksen JL, Baker M et al (2008) Common variation in the miR-659 binding-site of GRN is a major risk factor for TDP43-positive frontotemporal dementia. Hum Mol Genet 17:3631–3642. doi:10.1093/hmg/ddn257
35. Sampathu DM, Neumann M, Kwong LK et al (2006) Pathological heterogeneity of frontotemporal lobar degeneration with ubiquitin-positive inclusions delineated by ubiquitin immunohistochemistry and novel monoclonal antibodies. Am J Pathol 169:1343–1352. doi:10.2353/ajpath.2006.060438
36. Schwab C, Arai T, Hasegawa M, Yu S, McGeer PL (2008) Colocalization of transactivation-responsive DNA-binding protein 43 and huntingtin in inclusions of Huntington disease. J Neuropathol Exp Neurol 67(12):1159–1165
37. Sreedharan J, Blair IP, Tripathi VB et al (2008) TDP-43 mutations in familial and sporadic amyotrophic lateral sclerosis. Science 319:1668–1672. doi:10.1126/science.1154584
38. Tan CF, Eguchi H, Tagawa A et al (2007) TDP-43 immunoreactivity in neuronal inclusions in familial amyotrophic lateral sclerosis with or without SOD1 gene mutation. Acta Neuropathol 113:535–542. doi:10.1007/s00401-007-0206-9
39. Uryu K, Nakashima-Yasuda H, Forman MS et al (2008) Concomitant TAR-DNA-binding protein 43 pathology is present in Alzheimer disease and corticobasal degeneration but not in other tauopathies. J Neuropathol Exp Neurol 67:555–564. doi:10.1097/NEN.0b013e31817713b5
40. Van Deerlin VM, Leverenz JB, Bekris LM et al (2008) TARDBP mutations in amyotrophic lateral sclerosis with TDP-43 neuropathology: a genetic and histopathological analysis. Lancet Neurol 7:409–416. doi:10.1016/S1474-4422(08)70071-1
41. Vance C, Al-Chalabi A, Ruddy D et al (2006) Familial amyotrophic lateral sclerosis with frontotemporal dementia is linked to a locus on chromosome 9p13.2–21.3. Brain 129:868–875. doi:10.1093/brain/awl030
42. Watts GDJ, Wymer J, Kovach MJ et al (2004) Inclusion body myopathy associated with Paget disease of bone and frontotemporal dementia is caused by mutant valosin-containing protein. Nat Genet 36:377–381. doi:10.1038/ng1332
43. Yokoseki A, Shiga A, Tan CF et al (2008) TDP-43 mutation in familial amyotrophic lateral sclerosis. Ann Neurol 63:538–542. doi:10.1002/ana.21392

Acta Neuropathol (2009) 117:151–158
DOI 10.1007/s00401-008-0463-2

ORIGINAL PAPER

Accumulation of phosphorylated TDP-43 in brains of patients with argyrophilic grain disease

Hiroshige Fujishiro · Hirotake Uchikado · Tetsuaki Arai · Masato Hasegawa · Haruhiko Akiyama · Osamu Yokota · Kuniaki Tsuchiya · Takashi Togo · Eizo Iseki · Yoshio Hirayasu

Received: 24 October 2008 / Revised: 18 November 2008 / Accepted: 18 November 2008 / Published online: 28 November 2008

Abstract To determine whether TAR-DNA binding protein 43 (TDP-43) immunoreactivity was present in brains of argyrophilic grain disease (AGD), we immunohistochemically examined 15 cases of AGD (mean age at death: 84 years) using a panel of anti-TDP-43 antibodies, including both phosphorylation-independent and -dependent ones. Nine AGD cases (60%) showed TDP-43 immunoreactivities mainly in the limbic regions and lateral occipitotemporal cortex. TDP-43 positive structures included neuronal cytoplasmic inclusions, dystrophic neurites, glial cytoplasmic inclusions, grain-like dot-shaped structures, and neurofibrillary tangle (NFT)-like structures. The distribution of these TDP-43 positive structures was largely consistent with that of argyrophilic grains. Double-labeling confocal microscopy revealed, however, that many of phospho-TDP-43 positive structures were not colocalized with phospho-tau staining. Colocalization of phospho-TDP-43 and phospho-tau was observed only in part of neuronal cytoplasmic inclusions, grain-like structures and NFT-like structures. There were no differences in demographics, disease duration, brain weight, NFT Braak stage, or severity of amyloid burden between AGD cases with and without TDP-43-immunoreactivity. However, cases of AGD with TDP-43-immunoreactivity were assigned to higher AGD stages than those without TDP-43-immunoreactivity ($P < 0.05$). Furthermore, the TDP-43 pathology tended to be prominent in cases with severe grain pathology. The results of the present study indicate for the first time a high frequency of concomitant TDP-43 pathology in AGD, and suggest that abnormal accumulation of TDP-43 may be involved in the pathological process and disease progression of AGD.

Keywords TDP-43 · Phosphorylation · Neurofibrillary tangles · Argyrophilic grain · Tau

H. Fujishiro · H. Uchikado · T. Arai (✉) · H. Akiyama · O. Yokota
Department of Psychogeriatrics, Tokyo Institute of Psychiatry,
2-1-8 Kamikitazawa, Setagaya-ku, Tokyo 156-8585, Japan
e-mail: arai@prit.go.jp

H. Fujishiro · H. Uchikado · T. Togo · Y. Hirayasu
Department of Psychiatry, School of Medicine,
Yokohama City University, 3-9 Fukuura, Kanazawa-ku,
Yokohama, Kanagawa 236-0004, Japan

M. Hasegawa
Department of Molecular Neurobiology,
Tokyo Institute of Psychiatry, 2-1-8 Kamikitazawa,
Setagaya-ku, Tokyo 156-8585, Japan

K. Tsuchiya
Department of Laboratory Medicine and Pathology,
Tokyo Metropolitan Matsuzawa Hospital, 2-1-1 Kamikitazawa,
Setagaya-ku, Tokyo 156-0057, Japan

E. Iseki
Department of Psychiatry,
Juntendo Tokyo Koto Geriatric Medical Center,
Juntendo University School of Medicine,
3-3-20 Shinsuna, Koto-ku, Tokyo 136-0075, Japan

Introduction

Argyrophilic grain disease (AGD) was first described by Braak and Braak [3] in the brains of patients with adult-onset dementia. Subsequently, many studies have revealed that argyrophilic grains (AGs) are not rare pathological features among old demented patients [4]. Recently, Togo et al. have classified AGD as four-repeat tauopathy such as progressive supranuclear palsy (PSP) and corticobasal degeneration (CBD), based on morphological, biochemical, and genetic analyses [28, 29]. AGD is neuropathologically

characterized by the presence of small spindle- or comma-shaped silver stain positive structures, so-called argyrophilic grains, in the neuropil in the limbic area, which includes the hippocampus, the entorhinal and transentorhinal cortices and the cingulate cortex [3, 4, 7].

TAR-DNA-binding protein 43 (TDP-43) was first identified as a major component of the ubiquitin-positive inclusions in sporadic frontotemporal lobar degeneration with ubiquitinated inclusions (FTLD-U), familial FTLD-U with progranulin gene mutations, and sporadic amyotrophic lateral sclerosis (ALS) [2, 22]. Subsequent studies found that ubiquitin-positive inclusions in familial FTLD-U with valosin-containing protein gene [23], familial FTLD with motor neuron disease linked to chromosome 9p [6], and SOD-1-unrelated familial ALS were positive for TDP-43 [19, 27]. Recent findings of various missense mutations of TDP-43 gene in familial and sporadic ALS cases prove an essential role of TDP-43 abnormality in neurodegeneration [10, 18, 26, 31, 32]. These disorders are now referred to as TDP-43 proteinopathy [2, 22].

TDP-43 immunoreactivity, however, has also been detected in other neurodegenerative disorders, including Alzheimer's disease (AD), Lewy body disease (LBD), Pick's disease, Guamanian parkinsonism–dementia complex (G-PDC), Guamanian ALS (G-ALS), hippocampal sclerosis, and Huntington's disease [1, 2, 8, 9, 11, 13, 21, 25]. Uryu et al. [30] have recently reported that TDP-43 immunoreactive pathology was detected in 15% of corticobasal degeneration (CBD) cases, but not in other primary tauopathies including progressive supranuclear palsy (PSP). It is unknown, however, whether TDP-43 positive structures are present in AGD, which belongs to the primary tauopathies as well [28]. To address this issue, in the present study, we immunohistochemically investigated 15 cases of AGD using a panel of anti-TDP-43 antibodies. Here, we show a high frequency of TDP-43 positive structures, which are associated with the severity of tau-positive grain pathology in AGD.

Materials and methods

Materials

A total of 15 cases of AGD were employed in this study. The neuropathologic diagnosis was confirmed through standardized neuropathological examinations, which included staining with hematoxylin–eosin, Klüver–Barrera, methenamine–silver and modified Gallyas–Braak methods, in multiple cortical and subcortical areas. All cases were assigned to both a Braak stage of neurofibrillary tangles (NFTs) and an AGD stage based upon the distribution of NFTs and AGs seen by modified Gallyas–Braak staining (Fig. 1a) [5, 7, 24]. The degree of amyloid burden was evaluated based upon Consortium to Establish a Registry for Alzheimer Disease (CERAD) guidelines [20]. All cases were obtained from brain banks at the Department of Psychogeriatrics, Tokyo Institute of Psychiatry and at the Department of Psychiatry, Yokohama City University School of Medicine. All AGD cases (mean age 84.0 years; range 75–97 years; 7 females and 8 males) showed a NFT Braak stage below III, suggesting that they do not have concomitant AD.

Screening with TDP-43 immunohistochemistry

The presence and severity of TDP-43 immunoreactivity were assessed in the amygdala, entorhinal cortex, hippocampus, lateral occipitotemporal gyrus, and inferior temporal gyrus, using 10% formalin-fixed and paraffin-embedded 6 μm thick sections in all AGD cases. In four of 15 cases, 4% paraformaldehyde (PFA)-fixed and frozen sections in 30 μm thickness were also available. Sections were incubated with 0.5% H_2O_2 for 30 min to eliminate endogenous peroxidase activity in the tissue. After washing sections with 0.01 M phosphate-buffered saline (PBS, pH 7.4) containing 0.3% TritonX-100 (Tx-PBS) for 30 min, they were blocked with 10% normal serum, then incubated for 72 h at 4°C with a previously well characterized antibody specific for phosphorylated TDP-43 (pS409/410) in Tx-PBS containing 10% normal serum [12]. After three 10-min washes in Tx-PBS, sections were incubated in a biotinylated secondary antibody for 1 h, and then in avidin–biotinylated horseradish peroxidase complex (ABC Elite kit, Vector Laboratories, Burlingame, CA, US) for 1 h. The peroxidase labeling was visualized with 0.01% 3,3′-diaminobenzidine (DAB) as a chromogen. The sections were counterstained briefly with hematoxylin. When the presence of TDP-43 immunoreactivity was noted, additional regions including caudate nucleus, putamen, cingulate gyrus, insula, and frontal and parietal cortices were also immunohistochemically examined for TDP-43. Immunopositive structures to pS409/410 were confirmed with other several phosphorylation-dependent and -independent anti-TDP-43 antibodies (Table 1) [12, 16]. Tau-positive structures were examined by immunostaining with anti-phosphorylated tau (clone AT8; 1: 3000, Innogenetics, Ghent, Belgium) (Fig. 1b) and anti-four-repeat tau (RD4; 1: 100, Millipore, Billerica, MA) (Fig. 1c). Double labeling immunofluorescence for phosphorylated TDP-43 (pS409/410) and phosphorylated tau (clone AT8; 1: 3000, Innogenetics, Ghent, Belgium) was performed using fluorescein isothiocianate (FITC)- and tetramethylrhodamine isothiocyanate (TRITC)-conjugated secondary antibodies; sections were examined with a confocal laser microscope (LSM5 PASCAL; Carl Zeiss MicroImaging gmbh, Jena, Germany).

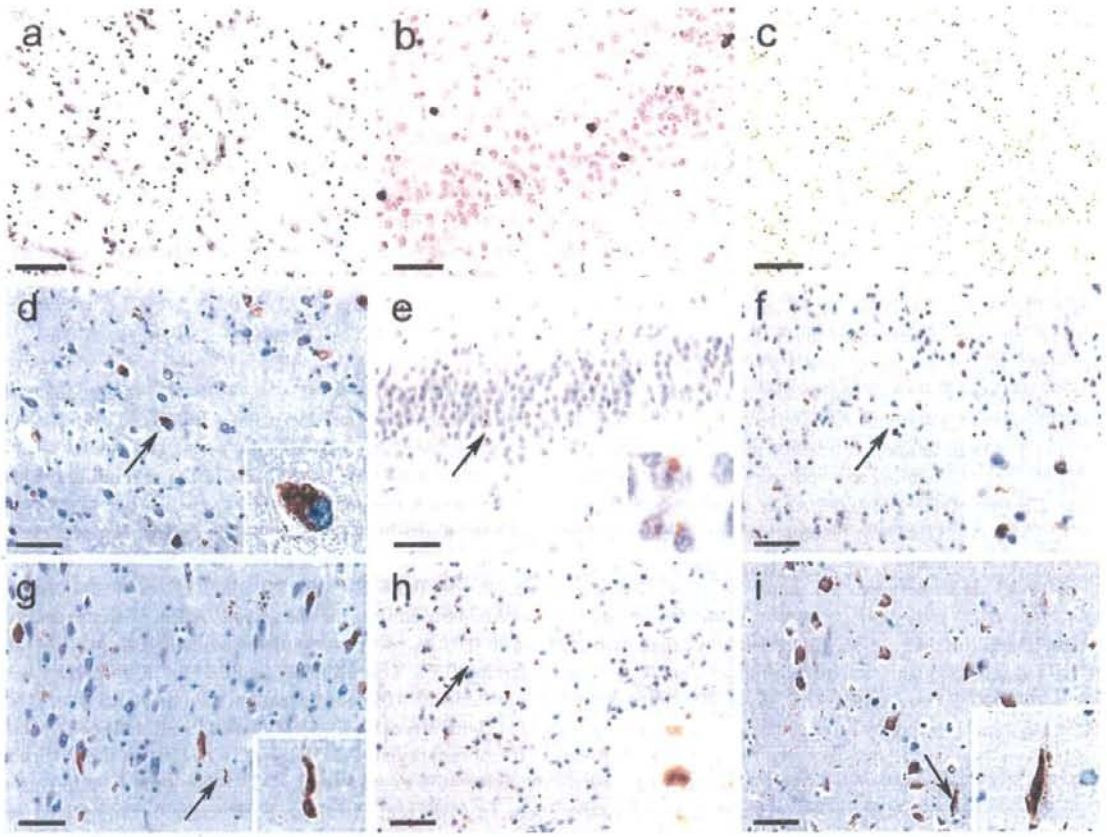

Fig. 1 Immunohistochemistry of argyrophilic grain disease using the phosphorylation-dependent anti-TDP-43 antibody (pS409/410). Modified Gallyas–Braak method (**a**) and immunostaining with anti-phosphorylated tau (**b**) and anti-four-repeat tau (**c**) show argyrophilic and tau-positive grains in amygdala (**a**) and CA1 region of hippocampus (**c**) and tau-positive neuronal cytoplasmic inclusions in the dentate granule cells (**b**). Phosphorylation-dependent TDP-43 immunohistochemistry reveals neuronal cytoplasmic inclusions (NCIs) (**d**, **e**), glial cytoplasmic inclusions (GCIs) (**f**) and dystrophic neurites (**g**). These are morphologically similar to TDP-43 positive structures observed in frontotemporal lobar degeneration with ubiquitinated inclusions (FTLD-U). Grain-like (**h**) and NFT-like (**i**) structures are also immunopositive. (**a**, **d**) amygdala, (**b**, **e**) dentate gyrus of hippocampus, (**c**, **i**) CA1 region of hippocampus, (**f**) lateral occipitotemporal cortex, (**g**) CA2 region of hippocampus, (**h**) entorhinal cortex. Each inset in a lower right corner represents a higher magnification of the region indicated by an *arrow* (*bars* 50 μm)

Table 1 Anti-TDP-43 antibodies used in this study

Antibody	Type	Antigen	Dilution
10782-2-AP (Protein Tech Group)	Rabbit	Recombinant protein (aa 1–260)	1:1,000
Anti-TDP43N [3–12]	Rabbit	EYIRVTEDENC (aa3–12)	1:1,000
pS409/410	Rabbit	CMDSKS(p)S(p)GWGM (aa 405–414)	1:1,000
pS403/404	Rabbit	NGGFGS(p)S(p)MDSKC (aa 398–408)	1:1,000
Anti-TDP43C (405–414)	Rabbit	CMDSKSSGWGM (aa 405–414)	1:1,000

Evaluation of severity and distribution of TDP-43 immunoreactivity in AGD

TDP-43 immunoreactive structures were examined on microscopic fields at 200× magnification in the amygdala, the entorhinal cortex, the striatum (putamen and caudate), the hippocampus (3 regions; CA1, CA2, and dentate gyrus), the cingulate gyrus, the insulated cortex, the lateral occipitotemporal cortex, and the inferior temporal cortex. TDP-43 immunoreactive structures were semi-quantitatively scored from (−) to (+++): (−) = absent; (+) = mild; (++) = moderate; (+++) = severe. TDP-43 immunoreactive

structures were separately evaluated as neuronal cytoplasmic inclusions (NCI), dystrophic neurites (DN) and glial cytoplasmic inclusions (GCI).

Statistical analyses

Data were analyzed with SigmaStat 3.5 (Systat Software, Inc., Point Richmond, CA, US), and the significance level was set at $P < 0.05$. To compare cases of AGD with and without TDP-43 immunoreactivity with respect to age at death, disease duration, brain weight, Braak NFT stage [5], CERAD plaque score [20], and AGD stage [7, 24], *t* test or Mann–Whitney Sum Rank Test was performed as appropriate. To compare cases of AGD with and without TDP-43 immunoreactivity, Fisher's exact test was performed with respect to sex ratio. According to CERAD criteria [20], amyloid burden was scored as follows; none: 0, sparse: 1, moderate: 2, frequent: 3. TDP-43 immunoreactivity was scored as follows; absence: 0, presence: 1. Relationships among pathological variables were assessed with Spearman's Rank Order Correlation.

Results

Distribution of TDP-43 immunoreactive structures and AGs

Prior to this study, we had produced several phosphorylation-specific anti-TDP-43 antibodies [12, 16]. These antibodies react only with abnormally deposited TDP-43 with no nuclear staining, making it easy for us to recognize abnormal findings. In this study, using these antibodies, we found various types of TDP-43 positive structures in nine of 15 AGD cases (60%). They include neuronal cytoplasmic inclusions, dystrophic neurites and glial cytoplasmic inclusions (Fig. 1d–g). In addition to these FTLD-U-like lesions, some grain-like structures were found to be positive for TDP-43 (Fig. 1h). Various amounts of TDP-43 immunoreactive NFT-like structures were also observed (Fig. 1i). There was no neuronal intranuclear inclusion in this series. These TDP-43 positive structures were mainly detected in the amygdala, entorhinal cortex, hippocampal CA1, subiculum and lateral occipitotemporal cortex. Of these regions, the amygdala and adjacent entorhinal cortex showed the most intense TDP-43 immunoreactivity. TDP-43 positive neuronal cytoplasmic inclusions in the dentate gyrus of the hippocampus, which is one of the features of FTLD-U, were observed in only two of nine cases with TDP-43 immunoreactivity.

The distribution and severity of TDP-43 immunoreactive structures were largely parallel with that of AGs, as detailed in Table 2. For instance, both TDP-43 positive structures and tau positive AGs were relatively confined to the amygdala and anterior parahippocampal gyrus in cases 1–5, and they extended to the temporal neocortices in cases eight and nine. Furthermore, cases 7–9 exhibited TDP-43 immunoreactive pathology in the pyramidal neurons in the CA2, where NFTs are common in AGD but not in AD [17]

Table 2 AGD staging and distribution of TDP-43-immunoreactive pathology

	AGD staging	AMY	Parahippocampal gyrus	Hippocampus			CIG	INS	OTC	ITC	CP
			(ant/post)	CA1	CA2	DG	(ant/post)	(ant/post)	(ant/post)	(ant/post)	
#1	I	NCI+, GCI+	NCI+, DN+, GCI+/0	NCI++	0	0	0/0	0/0	0/0	0/0	0
#2	I	NCI+, DN+	NCI+, GCI+/0	0	0	0	0/0	0/0	NCI++, GCI+/0	0/0	0
*#3	II	0	0	NCI+	0	0	0/0	0/0	0/0	0/0	0
#4	II	NCI+, GCI+	NCI+, GCI+/0	0	0	0	0/0	0/0	0/0	0/0	0
#5	II	NCI ++, GCI +	NCI++, GCI +/0	NCI++	0	0	0/0	0/0	NCI+, GCI+, DN+/0	0/0	0
#6	III	NCI+	NCI+, DN+, GCI+/DN+	NCI+	0	0	0/0	0/0	NCI+, GCI+, DN+/0	0/0	0
#7	III	NCI+++, GCI++	NCI+++, GCI++, DN+/NCI+++, GCI++, DN+	NCI++	NCI+	0	0/0	NCI+/0	NCI++, GCI++, DN+/NCI+	0/0	0
#8	III	NCI++, GCI +	NCI++, GCI+/NCI++	NCI++	NCI+, DN+	NCI+	NA	NCI+/0	NCI+/NCI+	NCI+/0	0
#9	IV	NCI++, DN++, GCI+	NCI+, DN++, GCI+/NCI+, DN+	NCI+	NCI+	NCI+	0/0	0/0	NCI+, DN++, GCI+/NCI+, DN++	DN+/0	0

AMY amygdala, *CIG* cingulated gyrus, *INS* insula, *OTC* occipitotemporal cortex, *ITC* inferior temporal cortex, *CP* caudate/putamen, *ant* anterior, *post* posterior, *NCI* neuronal cytoplasmic inclusions, *GCI* glial cytoplasmic inclusions, *DN* dystrophic neurites, *NA* not available, – absent, + mild, ++ moderate, +++ severe, *in this case (#3), there is a discrepancy of TDP-43 immunoreactivity between formalin-fixed paraffin-embedded sections and paraformaldehyde-fixed floating sections (see "Results"; Fig. 4)

(Fig. 1g). Finally, TDP-43 immunoreactivity tended to be more intense in anterior part of the hippocampus and parahippocampal gyrus than in posterior part of those in most cases. This pathological distribution was again in accordance with an AGs staging system that reflects an antero-posterior gradient in the putative progression of AGD [7, 24].

Colocalization of TDP-43 immunoreactive structures and tau positive structures

Double-labeling confocal microscopy revealed virtually no colocalization of phospho-tau and phospho-TDP-43 in the dentate gyrus of the hippocampus (Fig. 2a–c). In the entorhinal cortex and the amygdala, however, occasional colocalization of phospho-tau and phospho-TDP-43 was observed in the neuronal cytoplasmic inclusions and grain-like structures in neuropil (Fig. 2d–f). In neurons that showed cytoplasmic co-existence of both proteins, phospho-TDP-43 positive structures were sometimes separated from phospho-tau (Fig. 2g, h).

Confirmation of TDP-43 immunoreactivity through various methods

The staining patterns obtained with pS409/410, a phosphorylation-specific antibody (Fig. 1d–i), were almost same as those obtained with pS403/404, another phosphorylation-specific antibody (Fig. 3b, f). They stained only abnormal structures with no nuclear staining. Anti-TDP43C (405–414), a phosphorylation-independent C-terminal antibody, showed similar staining to those except for a weak staining of normal nuclei (Fig. 3c). Commercial antibody (10782-2-AP) and anti-TDP43N [3–12], a phosphorylation-independent N-terminal antibody, also stained abnormal structures with intense nuclear staining (Fig. 3a, d, e). Because of such nuclear staining, it was difficult to identify grain-like structures using these phosphorylation-independent antibodies.

In four cases for which both formalin-fixed paraffin-embedded sections and 4% PFA-fixed free-floating frozen sections were available, one case showed TDP-43 immunoreactivity. In this case, however, a significant difference of

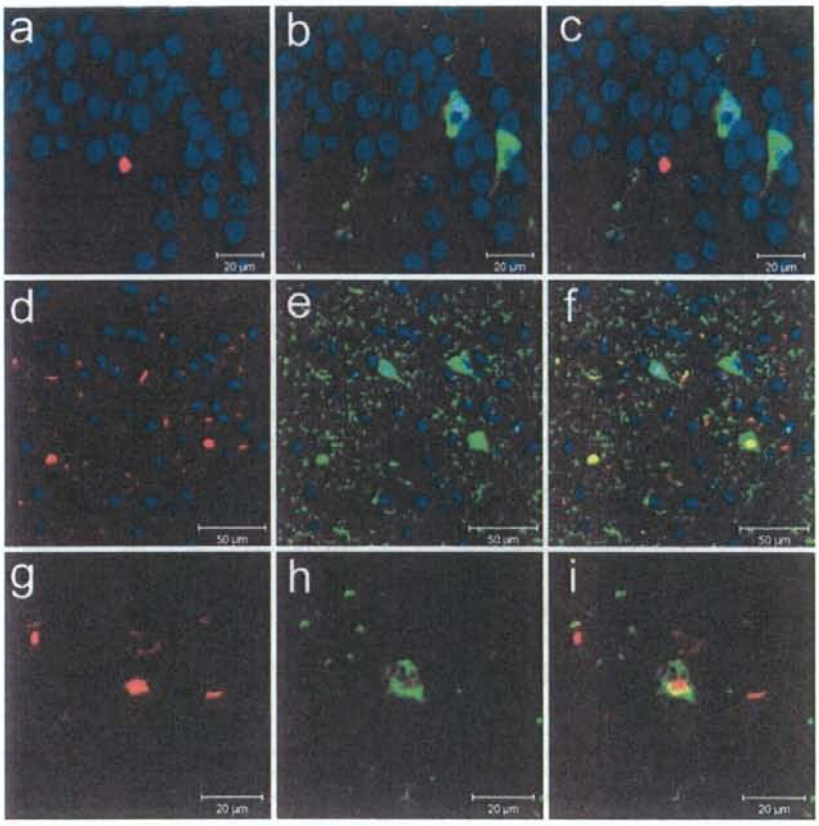

Fig. 2 Confocal double-immunofluorescence of phospho-TDP43 (**a**, **d**, **g**) and phospho-tau (**b**, **e**, **h**). Merged images are shown in **c**, **f** and **i**. In the granular cells in the dentate gyrus of the hippocampus, a TDP-43 positive neuronal cytoplasmic inclusion (*red* fluorescence in **a** and **c**) is not colocalized with tau labeling (*green* fluorescence in **b** and **c**). In the entorhinal cortex, small dot-like structures, short dystrophic neurites and round inclusions are immunopositive for TDP-43 (**d**), and a lot of grains and neurons are positive for tau (**e**). Partial colocalization is seen in some grain-like structures in the neuropil and neuronal cytoplasmic inclusions (*yellow* in **f**). Nuclei are stained with TO-PRO-3 (Invitrogen, Tokyo, Japan), producing a blue color. A higher magnification of co-existence of phospho-tau and phospho-TDP-43 seen in the same neurons (**g**–**i**). Most of phospho-TDP-43 positive structure (*red* in **g** and **h**) is separated from phospho-tau (*green* in **h** and **i**)

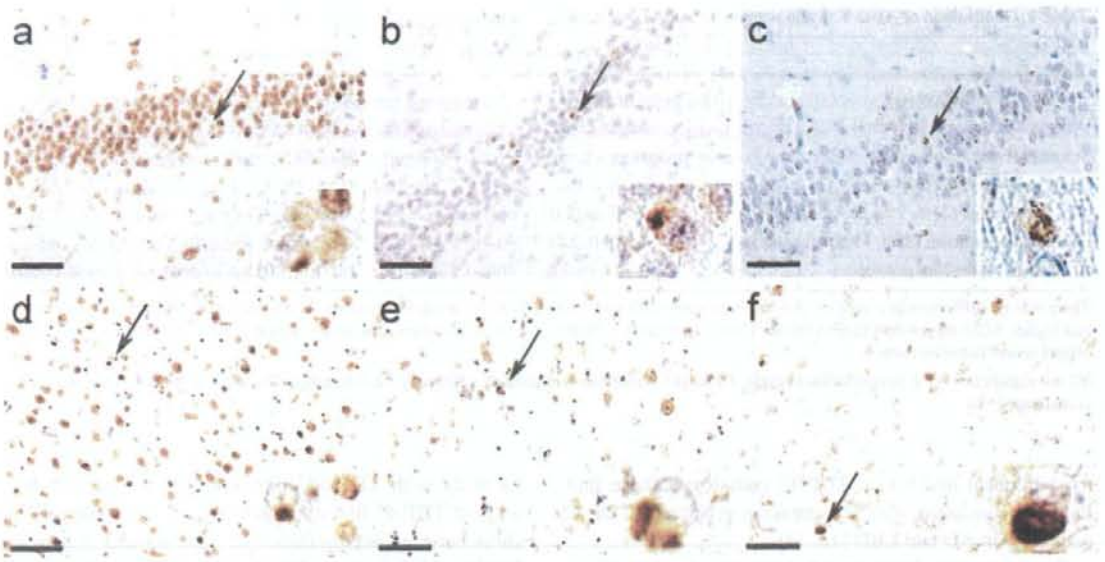

Fig. 3 Immunohistochemistry using a panel of anti-TDP-43 antibodies. Immunostaining of dentate gyrus of the hippocampus (**a–c**) and amygdala (**d–f**) using commercial phosphorylation-independent antibody (10782-2-AP, Protein Tech) (**a**, **d**), pS403/404 (**b**, **f**), anti-TDP43C (405–414) (**c**), and anti-TDP43N [3–12] (**e**). All antibodies positively stain neuronal cytoplasmic inclusions. Note that it is easier to recognize neuronal cytoplasmic inclusions by pS403/404 (**b**, **f**) and anti-TDP43C (405–414) (**c**) than by a commercial antibody to TDP-43 (**a**, **d**) and anti-TDP43 N [3–12] (**e**), which intensely stain normal nuclei. Each inset in a lower right corner represents a higher magnification of the region indicated by an *arrow* (*bars* 50 μm)

the immunoreactivity was observed between the sections. In free-floating sections, massive TDP-43 positive grain-like structures in the neuropil in the entorhinal cortex (Fig. 4a) and neuronal cytoplasmic inclusions in the dentate fascia (Fig. 4b) were recognized, while in paraffin-embedded sections, only occasional neuronal cytoplasmic inclusions were seen in CA1 of the hippocampus. This discrepancy of immunoreactivity may be due to methodological differences including a fixation and a treatment of brain tissues.

Relationship of TDP-43 immunoreactivity to demographics and pathological variables

There were no differences in age at death, disease duration, sex, brain weight, NFT Braak stage, or severity of amyloid burden between AGD cases with and without TDP-43 immunoreactivity. Clinical diagnoses are varied in both AGD cases with and without TDP-43 immunoreactivity: four senile dementia, one Alzheimer's disease, one vascular dementia, one Parkinson's disease with dementia, two schizophrenia in nine AGD cases with TDP-43 immunoreactivity, and one senile dementia, one alcoholic dementia, one dementia with Lewy bodies, one senile psychosis, one unclassified dementia, one schizophrenia in six AGD cases without TDP-43 immunoreactivity. There was no AGD case with clinical diagnosis of FTLD in this series. AGD cases with TDP-43-immunoreactivity had higher AGD stages than those without TDP-43 immunoreactivity ($P < 0.05$). The frequency of TDP-43 immunoreactivity was correlated with AGD stage ($r = 0.62$, $P = 0.01$), and with CERAD plaque scores ($r = -0.53$, $P = 0.03$), but not with NFT Braak stage ($r = 0.06$, $P = 0.80$).

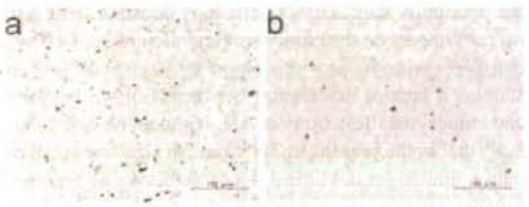

Fig. 4 Immunohistochemistry of free-floating sections of case #3 using pS409/410. **a** Massive grain-like or dot-like structures and short dystrophic neurites in the entorhinal cortex. **b** A lot of neuronal cytoplasmic inclusions in the dentate gyrus of the hippocampus

Discussion

By immunohistochemical examinations using a panel of phosphorylation-dependent and -independent antibodies to TDP-43, in this study, we demonstrated a high frequency (60%) of TDP-43 pathology in AGD cases for the first time. The limbic regions, especially the amygdala and the anterior part of the parahippocampal gyrus, showed the

Table 3 Comparison of AGD with and without TDP43-immunoreactive pathology

	TDP-43 positive ($N = 9$)	TDP-43 negative ($N = 6$)	P value
Age at death ± SD (years)	82.8 ± 6.7	85.8 ± 8.9	NS
Disease duration ± SD, (years)	5.5 ± 3.0 ($N = 6$)	7.2 ± 3.4 ($N = 4$)	NS
Sex ratio (F/M)	4/5	3/3	NS
Brain weight ± SD (gm)	1124 ± 102	1121 ± 155	NS
NFT Braak stage (25th, 75th percentile)	2.0(1.25, 2.0)	2.0 (1.0, 2.75)	NS
CERAD plaque score (25th, 75th percentile)	2.0 (0.0, 2.0)	2.5 (2.0, 3.0)	NS
AGD stage (25th, 75th percentile)	2.0 (1.75, 3.0)	1.0 (1.0, 1.0)	$P < 0.05$

There was no difference in demographics between cases with and without TDP-43 immunoreactivity. AGD cases with TDP-43 immunoreactivity had higher AGD stages than those without TDP-43 immunoreactivity ($P < 0.05$), but there was no difference in NFT Braak stages and CERAD plaque scores between them

NS not significant, *NFT* neurofibrillary tangle, *CERAD* Consortium to Establish a Registry for Alzheimer Disease Guidelines, *AGD* argyrophilic grain disease

most frequent and severe TDP-43 pathology. These findings are consistent with the previous reports of TDP-43 pathology in AD and LBD [13, 14].

Recent reports have revealed various degrees of co-occurrence of TDP-43 immunoreactivity in a variety of neurodegenerative disorders, including AD, LBD, CBD, Guamanian ALS/PDC and Huntington's disease [1, 9, 11, 13, 21, 25, 30]. Amador–Ortiz reported that 20–30% of AD and 70% of hippocampal sclerosis had TDP-43 immunoreactivity [1]. All AGD cases employed in this study did not fulfill the pathological criteria of AD, and there is no significant difference of Braak staging between cases with TDP-43 immunoreactivity and those without TDP-43 immunoreactivity (Table 3). Although only one AGD case with hippocampal sclerosis was included in our series, that case showed no TDP-43 immunoreactivity. Thus, it is unlikely that a high frequency of TDP-43 pathology in this AGD series is due to concurrent AD or hippocampal sclerosis.

In this AGD series, although the concomitant TDP-43 pathology was the most severe in the limbic structures, many cases showed the extension of TDP-43 pathology into the temporal neocortices. It is currently unknown if this represents concurrent primary pathological process of FTLD-U, or a secondary change occurring in susceptible neuronal populations. At least, a simple coincidence of FTLD-U and AGD seems unlikely based on our findings as follows. First, the frequency of TDP-43 positive neuronal cytoplasmic inclusions in the dentate gyrus, which are one of the pathological hallmarks of FTLD-U, is low (22%) in our AGD cases with TDP-43 immunoreactivity. Second, TDP-43 positive grain-like structures found in our AGD cases have not been reported in FTLD-U brains so far. Third, parallel distribution of TDP-43 positive structures and tau positive AGs and a higher AGD stages in cases with TDP-43 immunoreactivity than in those without TDP-43 immunoreactivity suggest some relationships between accumulation of TDP-43 and that of tau. Double label immunofluorescence microscopy revealed partial colocalization of phospho-tau and phospho-TDP-43 in grain-like structures and neuronal cytoplasmic inclusions in this study. Such partial colocalization of tau and TDP-43 is consistent with that previously reported in AD, LBD, Guamanian PDC and CBD [1, 2, 8, 11, 13, 21]. Although these findings may not suggest a direct interaction between tau and TDP-43, there may be common factors or mechanisms that affect the conformation or modification of both proteins, leading to their intracellular accumulation.

Ikeda et al. [15] reported that the clinical features of AGD consist of personality changes characterized by emotional disorder with aggression or ill temper and relatively preserved cognitive function. These clinical features are also observed in FTLD. In this study, however, none of AGD cases, including the case with massive TDP-43 pathology (Fig. 4), had a clinical diagnosis of FTLD. Moreover, there was no significant difference in demographics, including age at death, disease duration, sex and brain weight, between AGD cases with TDP-43 pathology and those without TDP-43 pathology. These findings suggest the possibility that TDP-43 pathology does not have a significant impact on the clinical presentation of AGD. This is consistent with the previous report by Uryu et al. [30] that showed a lack of association between TDP-43 pathology and clinical manifestations in AD. It should be noted, however, that in the present study, a sample size was small and only a limited set of clinical manifestations was examined. Further studies using more detailed associations with larger data sets on behavioral impairments in AGD should be performed.

Acknowledgments The assistance of Kyoko Suzuki, Chie Haga and Hiromi Kondo for histologic and immunohistochemistry studies is greatly appreciated. We are grateful to Dr. de Silva for generous supply of RD4 antibody.

References

1. Amador-Ortiz C, Lin WL, Ahmed Z et al (2007) TDP-43 immunoreactivity in hippocampal sclerosis and Alzheimer's disease. Ann Neurol 61:435–445
2. Arai T, Hasegawa M, Akiyama H et al (2006) TDP-43 is a component of ubiquitin-positive tau-negative inclusions in frontotemporal lobar degeneration and amyotrophic lateral sclerosis. Biochem Biophys Res Commun 351:602–611
3. Braak H, Braak E (1987) Argyrophilic grains: characteristic pathology of cerebral cortex in cases of adult onset dementia without Alzheimer changes. Neurosci Lett 76:124–127
4. Braak H, Braak E (1989) Cortical and subcortical argyrophilic grains characterize a disease associated with adult onset dementia. Neuropathol Appl Neurobiol 15:13–26
5. Braak H, Braak E (1991) Neuropathological stageing of Alzheimer-related changes. Acta Neuropathol 82:239–259
6. Cairns NJ, Neumann M, Bigio EH et al (2007) TDP-43 in familial and sporadic frontotemporal lobar degeneration with ubiquitin inclusions. Am J Pathol 171:227–240
7. Ferrer I, Santpere G, van Leeuwen FW (2008) Argyrophilic grain disease. Brain 131:1416–1432
8. Freeman SH, Spires-Jones T, Hyman BT, Growdon JH, Frosch MP (2008) TAR-DNA binding protein 43 in Pick disease. J Neuropathol Exp Neurol 67:62–67
9. Geser F, Winton MJ, Kwong LK et al (2008) Pathological TDP-43 in parkinsonism-dementia complex and amyotrophic lateral sclerosis of Guam. Acta Neuropathol 115:133–145
10. Gitcho MA, Baloh RH, Chakraverty S et al (2008) TDP-43 A315T mutation in familial motor neuron disease. Ann Neurol. doi:10.1002/ana.21344
11. Hasegawa M, Arai T, Akiyama H et al (2007) TDP-43 is deposited in the Guam parkinsonism-dementia complex brains. Brain 130:1386–1394
12. Hasegawa M, Arai T, Nonaka T et al (2008) Phosphorylated TDP-43 in frontotemporal lobar degeneration and amyotrophic lateral sclerosis. Ann Neurol 64:60–70
13. Higashi S, Iseki E, Yamamoto R et al (2007) Concurrence of TDP-43, tau and alpha-synuclein pathology in brains of Alzheimer's disease and dementia with Lewy bodies. Brain Res 1184:284–294
14. Hu WT, Josephs KA, Knopman DS et al (2008) Temporal lobar predominance of TDP-43 neuronal cytoplasmic inclusions in Alzheimer disease. Acta Neuropathol 116:215–220
15. Ikeda K, Akiyama H, Arai T et al (2000) Clinical aspects of argyrophilic grain disease. Clin Neuropathol 19:278–284
16. Inukai Y, Nonaka T, Arai T et al (2008) Abnormal phosphorylation of Ser409/410 of TDP-43 in FTLD-U and ALS. FEBS Lett 582:2899–2904
17. Ishizawa T, Ko LW, Cookson N, Davias P, Espinoza M, Dickson DW (2002) Selective neurofibrillary degeneration of the hippocampal CA2 sector is associated with four-repeat tauopathies. J Neuropathol Exp Neurol 61:1040–1047
18. Kabashi E, Valdmanis PN, Dion P et al (2008) TARDBP mutations in individuals with sporadic and familial amyotrophic lateral sclerosis. Nat Genet 40:572–574
19. Mackenzie IR, Bigio EH, Ince PG et al (2007) Pathological TDP-43 distinguishes sporadic amyotrophic lateral sclerosis from amyotrophic lateral sclerosis with SOD1 mutations. Ann Neurol 61:427–434
20. Mirra SS, Heyman A, McKeel D et al (1991) The Consortium to Establish a Registry for Alzheimer's Disease (CERAD). Part II. Standardization of the neuropathologic assessment of Alzheimer's disease. Neurology 41:479–486
21. Nakashima-Yasuda H, Uryu K, Robinson J et al (2007) Co-morbidity of TDP-43 proteinopathy in Lewy body related diseases. Acta Neuropathol 114:221–229
22. Neumann M, Sampathu DM, Kwong LK et al (2006) Ubiquitinated TDP-43 in frontotemporal lobar degeneration and amyotrophic lateral sclerosis. Science 314:130–133
23. Neumann M, Mackenzie IR, Cairns NJ et al (2007) TDP-43 in the ubiquitin pathology of frontotemporal dementia with VCP gene mutations. J Neuropathol Exp Neurol 66:152–157
24. Saito Y, Ruberu NN, Sawabe M et al (2004) Staging of argyrophilic grains: an age-associated tauopathy. J Neuropathol Exp Neurol 63:911–918
25. Schwab C, Arai T, Hasegawa M, Yu S, McGeer PL (2008) Colocalization of TDP-43 and huntingtin in inclusions of Huntington's disease. J Neuropathol Exp Neurol (in press)
26. Sreedharan J, Blair IP, Tripathi VB et al (2008) TDP-43 mutations in familial and sporadic amyotrophic lateral sclerosis. Science 319:1668–1672
27. Tan CF, Eguchi H, Tagawa A et al (2007) TDP-43 immunoreactivity in neuronal inclusions in familial amyotrophic lateral sclerosis with or without SOD1 gene mutation. Acta Neuropathol 113:535–542
28. Togo T, Sahara N, Yen SH et al (2002) Argyrophilic grain disease is a sporadic 4-repeat tauopathy. J Neuropathol Exp Neurol 61:547–556
29. Togo T, Cookson N, Dickson DW (2002) Argyrophilic grain disease: neuropathology, frequency in a dementia brain bank and lack of relationship with apolipoprotein E. Brain Pathol 12:45–52
30. Uryu K, Nakashima-Yasuda H, Forman MS et al (2008) Concomitant TAR-DNA-binding protein 43 pathology is present in Alzheimer disease and corticobasal degeneration but not in other tauopathies. J Neuropathol Exp Neurol 67:555–564
31. Van Deerlin VM, Leverenz JB, Bekris LM et al (2008) TARDBP mutations in amyotrophic lateral sclerosis with TDP-43 neuropathology: a genetic and histopathological analysis. Lancet Neurol 7:409–416
32. Yokoseki A, Shiga A, Tan CF et al (2008) TDP-43 mutation in familial amyotrophic lateral sclerosis. Ann Neurol 63:538–542

FEBS Letters 583 (2009) 394–400

FEBS Letters

journal homepage: www.FEBSLetters.org

Phosphorylated and ubiquitinated TDP-43 pathological inclusions in ALS and FTLD-U are recapitulated in SH-SY5Y cells

Takashi Nonaka [a,*], Tetsuaki Arai [b], Emanuele Buratti [c], Francisco E. Baralle [c], Haruhiko Akiyama [b], Masato Hasegawa [a,*]

[a] Department of Molecular Neurobiology, Tokyo Institute of Psychiatry, Tokyo Metropolitan Organization for Medical Research, 2-1-8 Kamikitazawa, Setagaya-ku 156-8585, Tokyo, Japan
[b] Department of Psychogeriatrics, Tokyo Institute of Psychiatry, Tokyo Metropolitan Organization for Medical Research, 2-1-8 Kamikitazawa, Setagaya-ku 156-8585, Tokyo, Japan
[c] International Centre for Genetic Engineering and Biotechnology, 34012 Trieste, Italy

ARTICLE INFO

Article history:
Received 31 October 2008
Revised 10 December 2008
Accepted 11 December 2008
Available online 25 December 2008

Edited by Barry Halliwell

Keywords:
TDP-43
FTLD-U
ALS
Phosphorylation
Ubiquitination

ABSTRACT

We report phosphorylated and ubiquitinated aggregates of TAR DNA binding protein of 43 kDa (TDP-43) in SH-SY5Y cells similar to those in brains of amyotrophic lateral sclerosis (ALS) and frontotemporal lobar degeneration with ubiquitinated inclusions (FTLD-U). Two candidate sequences for the nuclear localization signal were examined. Deletion of residues 78–84 resulted in cytoplasmic localization of TDP-43, whereas the mutant lacking residues 187–192 localized in nuclei, forming unique dot-like structures. Proteasome inhibition caused these to assemble into phosphorylated and ubiquitinated TDP-43 aggregates. The deletion mutants lacked the exon skipping activity of cystic fibrosis transmembrane conductance regulator (CFTR) exon 9. Our results suggest that intracellular localization of TDP-43 and proteasomal function may be involved in inclusion formation and neurodegeneration in TDP-43 proteinopathies.

1. Introduction

Frontotemporal lobar degeneration with ubiquitinated inclusions (FTLD-U) and amyotrophic lateral sclerosis (ALS) are well-known neurodegenerative disorders. FTLD is the second most common form of cortical dementia in the population below the age of 65 years [1]. ALS is the most common of the motor neuron diseases, being characterized by progressive weakness and muscular wasting, resulting in death within a few years. Ubiquitin (Ub)-positive inclusions were found as a pathological hallmark in brains of patients with FTLD-U and ALS, as well as in Alzheimer's disease (AD) and Parkinson's disease (PD). Recently, TAR DNA binding protein of 43 kDa (TDP-43) has been identified to be a major protein component of ubiquitin-positive inclusions in FTLD-U and ALS brains [2,3]. TDP-43 was first identified as a cellular factor that binds to the TAR DNA of HIV type 1 [4], and was also identified independently as part of a complex involved in inhibition of the splicing of the cystic fibrosis transmembrane conductance regulator (CFTR) gene [5]. TDP-43 aggregates in neuronal cytoplasm and nuclei in a variety of neurodegenerative disorders, which are now collectively referred to as TDP-43 proteinopathies. For understanding molecular pathogenesis and evidence-based therapies for TDP-43 proteinopathies, it is necessary to study the molecular mechanisms of aggregation of TDP-43.

To elucidate these issues, in this study, we have established the cellular models for intracellular aggregates of TDP-43 similar to those in brains of TDP-43 proteinopathies patients. Expression of deletion mutants of TDP-43 lacking two candidate sequences for the nuclear localization signal (NLS), residues 78–84 or 187–192, resulted in the formation of Ub- and phosphorylated TDP-43-positive cytoplasmic inclusions in the presence of a proteasome inhibitor. These results suggest that intracellular localization of TDP-43 and proteasomal function may be involved in the pathological process of TDP-43 proteinopathies.

Abbreviations: FTLD-U, frontotemporal lobar degeneration with ubiquitinated inclusions; ALS, amyotrophic lateral sclerosis; Ub, ubiquitin; TDP-43, TAR DNA binding protein of 43 kDa; CFTR, cystic fibrosis transmembrane conductance regulator; NLS, nuclear localization signal; TX, Triton X-100; Sar, Sarkosyl.

* Corresponding authors. Fax: +81 3 3329 8035 (T. Nonaka).
E-mail addresses: nonakat@prit.go.jp (T. Nonaka), masato@prit.go.jp (M. Hasegawa).

0014-5793/$34.00 © 2008 Federation of European Biochemical Societies. Published by Elsevier B.V. All rights reserved.
doi:10.1016/j.febslet.2008.12.031

2. Materials and methods

2.1. Construction of plasmids

The PCR product of the open-reading frame of human TDP-43 using pRc-CMV-TDP-43 as a template was subcloned into the mammalian expression vector pcDNA3 (Invitrogen) using restriction sites BamH I and Xba I, creating pcDNA3-TDP-43. To construct plasmids of the deletion mutants, we used a site-directed mutagenesis kit (Strategene). PCR was performed using the forward primer (5′-GTATGTTGTCAACTATATGGATGAGACAGATGC-3′) and the reverse primer (5′-GCATCTGTCTCATCCATATAGTTGACAACATAC-3′) for the deletion mutant of 78–84 residues (ΔNLS), and the forward primer (5′-GCAAAGCCAAGATGAGGTGTTTGTGGGGCGC-3′) and the reverse primer (5′-GCGCCCCACAAACACCTCATCTTGGCTTTGC-3′) for the deletion mutant of 187–192 residues (Δ187–192), with pcDNA3-TDP-43 as a template, respectively. For the construction of the double-deletion mutant ΔNLS&187–192, PCR was performed using the forward primer (5′-GCAAAGCCAAGATGAGGTGTTTGTGGGGCGC-3′) and the reverse primer (5′-GCGCCCCACAAACACCTCATCTTGGCTTTGC-3′) with pcDNA3-TDP-43ΔNLS as a template.

The reporter plasmid pSPL3-CFTR9 was constructed as follows. Healthy human genomic DNA (a gift from Dr. Makoto Arai, Tokyo Institute of Psychiatry, Japan) was subjected to PCR with the use of the forward primer (5′-CGGAATTCACTTGATAATGGGCAAATATC-3′) and the reverse primer (5′-CCCTCGAGCTCGCCATGTGCAAGATACAG-3′), containing EcoR I and Xho I sites, respectively. The genomic region containing 221 bp of intron 8, the entire exon 9 (183 bp), and 266 bp of intron 9 of the human CFTR gene was amplified and digested with the two restriction enzymes, followed by ligation into pSPL3 (Life Technologies), affording the plasmid pSPL3-CFTR9. All constructs were verified by DNA sequencing.

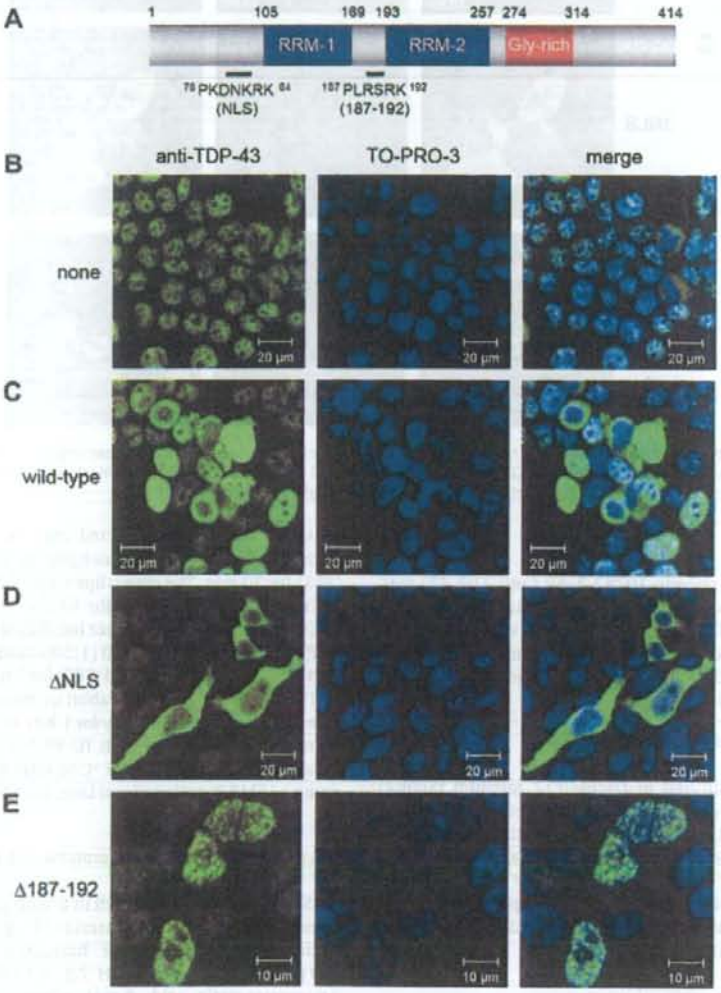

Fig. 1. Subcellular localization of wild-type and mutant TDP-43 in SH-SY5Y cells. (A) Schematic diagram of the structural domains of TDP-43. RNA recognition motifs (RRM-1 and -2: blue) and glycine-rich domain (Gly-rich: red) are shown. (B–E) Immunostaining of untransfected SH-SY5Y cells (B) and cells 72 h post transfection with wild-type TDP-43 (C), ΔNLS (Δ78–84) TDP-43 (D), and Δ187–192 TDP-43 (E) with anti-TDP-43 antibody (Left panel, green), nuclear staining by TO-PRO-3 (middle panel, blue) and the merged image (right panel) are shown.

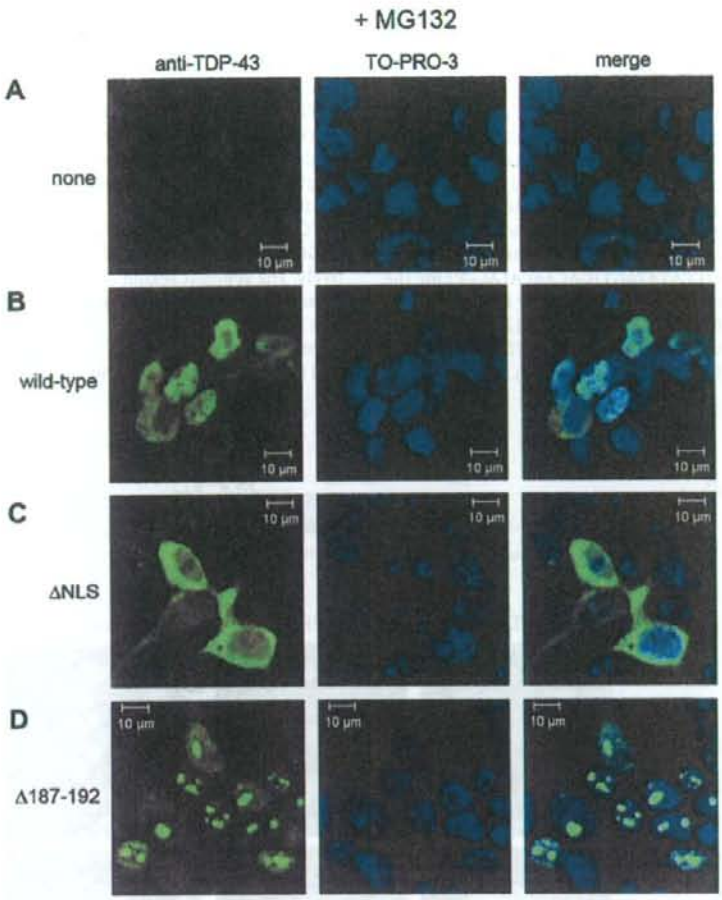

Fig. 2. Expression of mutant TDP-43 followed by proteasome inhibition with MG132 results in the formation of intranuclear inclusions. Immunostaining of untransfected cells (A) and cells 72 h post transfection with wild-type TDP-43 (B), ΔNLS (C), and Δ187–192 (D) followed by MG132 treatment (20 μM for 6 h) with anti-TDP-43 antibody (left panel, green), nuclear staining by TO-PRO-3 (middle panel, blue) and merged image (right panel).

2.2. Antibodies

A polyclonal TDP-43 antibody 10782-1-AP (anti-TDP-43) was purchased from ProteinTech Group Inc. A polyclonal antibody specific for phosphorylated TDP-43 (anti-pS409/410) was prepared as described [6]. Anti-ubiquitin monoclonal antibody (mAb), MAB1510, was purchased from Chemicon. Monoclonal anti-HA clone HA-7 were obtained from Sigma.

2.3. Cell culture and expression of plasmids

SH-SY5Y cells were cultured in DMEM/F12 medium (Sigma) supplemented with 10% (v/v) fetal calf serum, penicillin–streptomycin–glutamine (Gibco), and MEM non-essential amino acids solution (Gibco). Cells were then transfected with expression plasmids using FuGENE6 (Roche) according to the manufacturer's instructions. In the proteasome inhibition experiments, final 1 μM MG132 (Peptide institute) in DMSO was added to the culture medium, and incubated overnight.

2.4. Confocal immunofluorescence microscopy

SH-SY5Y cells were grown on a coverslip (15 × 15 mm) and transfected with expression vector (1 μg). After incubation for the indicated time, the transfected cells on the coverslips were fixed with 4% (w/v) paraformaldehyde in phosphate-buffered saline (PBS) for 30 min. The coverslips were then incubated with 0.2% (v/v) Triton X-100 (TX) in PBS for 10 min. After blocking for 30 min in 5% (w/v) BSA in PBS, cells were incubated with anti-phosphorylated TDP-43 antibody, pS409/410 (1:500 dilution), anti-TDP-43 (1:500), anti-Ub (1:500) or anti-HA (1:500) for 1 h at 37 °C, followed by FITC- or TRITC-labeled goat anti-rabbit or-mouse IgG (Sigma, 1:500 dilution) as a secondary antibody for 1 h at 37 °C. After washing, the cells were further incubated with TO-PRO-3 (Molecular Probes, 1:3000 dilution in PBS) for 1 h at 37 °C to stain nuclear DNA, and analyzed using a LSM5 Pascal confocal laser microscope (Carl Zeiss).

2.5. Sequential extraction of proteins and immunoblotting

SH-SY5Y cells were grown in 6-well plates and transfected transiently with expression plasmids (1 μg). After incubation for the indicated time, cells were harvested and lysed in TS buffer [50 mM Tris–HCl buffer, pH 7.5, 0.15 M NaCl, 5 mM ethylenediaminetetraacetic acid, 5 mM ethylene glycol bis(β-aminoethyl ether)-*N,N,N,N*-tetraacetic acid, and protease inhibitor cocktail (Roche)]. Lysates were centrifuged at 290,000×*g* for 20 min at 4 °C, and the supernatant was recovered as the TS-soluble fraction.

TS-insoluble pellets were lysed in TS buffer containing 1% (v/v) TX, and centrifuged at 290,000×g for 20 min at 4 °C. The supernatant was collected as TX-soluble fraction. TX-insoluble pellets were further sonicated in TS buffer containing 1% (w/v) Sarkosyl (Sar), and incubated for 30 min at 37 °C. The mixtures were centrifuged at 290,000×g for 20 min at room temperature, and the supernatant was recovered as the Sar-soluble fraction. The remaining pellets (insoluble in Sar) were lysed in SDS-sample buffer and heated for 5 min.

Each sample (10 or 20 μg) was separated by 12% (v/v) SDS–PAGE using Tris–glycine buffer system, and proteins were transferred onto polyvinylidene difluoride membrane (Millipore). The blots were incubated overnight with the indicated primary antibody at an appropriate dilution (1:1000–3000) at room temperature, followed by the incubation with a biotin-labeled secondary antibody. Signals were detected using an ABC staining kit (Vector).

2.6. CFTR exon 9 skipping assay

Cos-7 cells in 6-well plates were transfected with 0.5 μg of the reporter plasmid pSPL3-CFTR9 plus 1 μg of pcDNA3 plasmid encoding wild-type or its mutants, using FuGENE6. The cells were harvested 48 h post transfection, and total RNA was extracted with TRIzol (Invitrogen). The cDNA was synthesized from 1 μg of total RNA with the use of the Superscript II system (Invitrogen). Primary and secondary PCRs were carried out according to the instruction manual of the exon trapping system (Life Technologies).

3. Results

3.1. Effect of deletion of two candidate NLS in TDP-43

Amino acid sequence containing proline followed by a cluster of basic amino acids is known to be typical NLS. We found two such sequences in TDP-43, PKDNKRK (residues 78–84) and PLRSRK (residues 187–192) (Fig. 1A). To examine whether these sequences function as the NLS, we constructed corresponding deletion mutants of TDP-43 and expressed them in SH-SY5Y cells. We employed non-tagged TDP-43 plasmid for expression in cultured cells, since expression of hemagglutinin (HA)-tagged TDP-43 in SH-SY5Y cells caused formation of inclusion-like structures (Fig. S1), suggesting that addition of the epitope tag to the N-terminus may affect the conformation of TDP-43 and promote non-specific aggregate formation.

Endogenous TDP-43 expressed in the nucleus (Fig. 1B). Similar but stronger nuclear TDP-43 staining was observed in cells expressing wild-type TDP-43 (Fig. 1C), as compared with non-transfected cells (Fig. 1B). When the deletion mutant lacking residues 78–84 (ΔNLS) was transiently expressed, strong TDP-43 signals were detected in cytoplasm (Fig. 1D). This is reasonable because the sequence of 78–84 contains a part of the bipartite NLS in TDP-43 recently identified by Winton et al. [7].

When the deletion mutant lacking residues 187–192 (Δ187–192) was expressed, on the other hand, the mutant protein formed dot-like structures in nuclei (Fig. 1E). This observation suggests that this sequence does not function as a NLS.

3.2. Formation of intracellular TDP-43 inclusions in cultured SH-SY5Y cells

Impaired Ub–proteasome system has been suggested in some forms of neurodegenerative disease [8], and TDP-43 is indeed ubiquitinated in the brains of patients with FTLD-U or ALS [3]. To examine whether impaired Ub–proteasome system is involved in inclusion formation, we treated cells transfected with TDP-43 wild-type or deletion mutants with a proteasome inhibitor, MG132. In immunocytochemistry using phosphorylation-independent anti-TDP-43 antibody, no obvious change in the localization of TDP-43 was observed in mock cells (Fig. 2A), or in cells transfected with wild-type (Fig. 2B) or ΔNLS mutant (Fig. 2C) after MG132 treatment, as compared to those without MG132 (Fig. 1). In contrast, many round nuclear inclusions were generated in cells transfected with Δ187–192 mutant after MG132 treatment (Fig. 2D: ~12% of inclusion-positive cells).

Fig. 3 revealed the results of double immunostaining using anti-pS409/410, phosphorylation-dependent anti-TDP-43 antibody [6], and anti-Ub antibody. Cells expressing wild-type TDP-43 showed

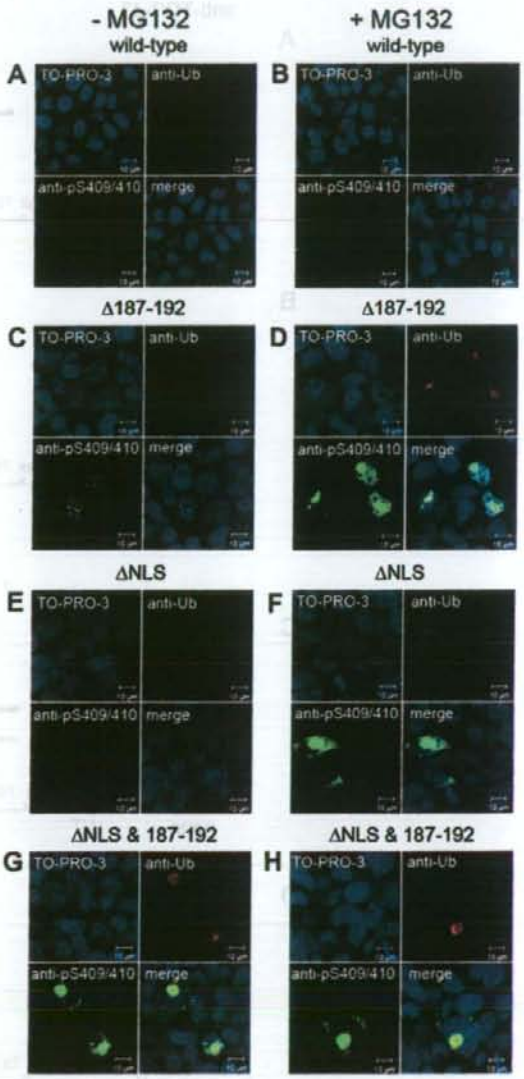

Fig. 3. Immunocytochemical analyses of intracellular inclusion-like structures formed in cells transfected with deletion mutants of TDP-43. SH-SY5Y cells 72 h post transfection with wild-type, (A and B), Δ187–192 (C and D), ΔNLS (E and F), and ΔNLS&187–192 (G and H) before (A, C, E, G) and after (B, D, F, H) treatment with MG132 (20 μM for 6 h) were stained with a phosphorylation-specific antibody, anti-pS409/410 (green), anti-ubiquitin (Ub: red) antibodies, and TO-PRO-3 (blue).

no immunoreactivity for anti-pS409/410 and anti-Ub antibodies in the presence or absence of MG132 (Fig. 3A and B). Cells transfected with Δ187–192 showed small dot-like structures positive for anti-pS409/410 antibody but negative for anti-Ub antibody without MG132 treatment (Fig. 3C). Cells transfected with Δ187–192 after the MG132 treatment contained inclusion-like structures in nuclei that were intensely labeled with both antibodies (Fig. 3D: ~8% of inclusion-positive cells). Relatively large inclusions (~5 μm) were immunopositive for both antibodies, while small ones (<1 μm) were positive for only phospho-specific TDP-43 antibody, suggesting that abnormal phosphorylation of TDP-43 is an early event in the process of inclusion formation.

Cells transfected with ΔNLS showed no immunoreactivity without MG132 treatment (Fig. 3E), but showed formation of cytoplasmic inclusions positive for both anti-pS409/410 and anti-Ub after MG132 treatment (Fig. 3F: ~10% of inclusion-positive cells). Furthermore, cells transfected with mutant TDP-43 lacking both the NLS and residues 187–192, named ΔNLS&187–192, formed intracellular round inclusion-like structures positive for both anti-pS409/410 and anti-Ub antibodies, independently of treatment

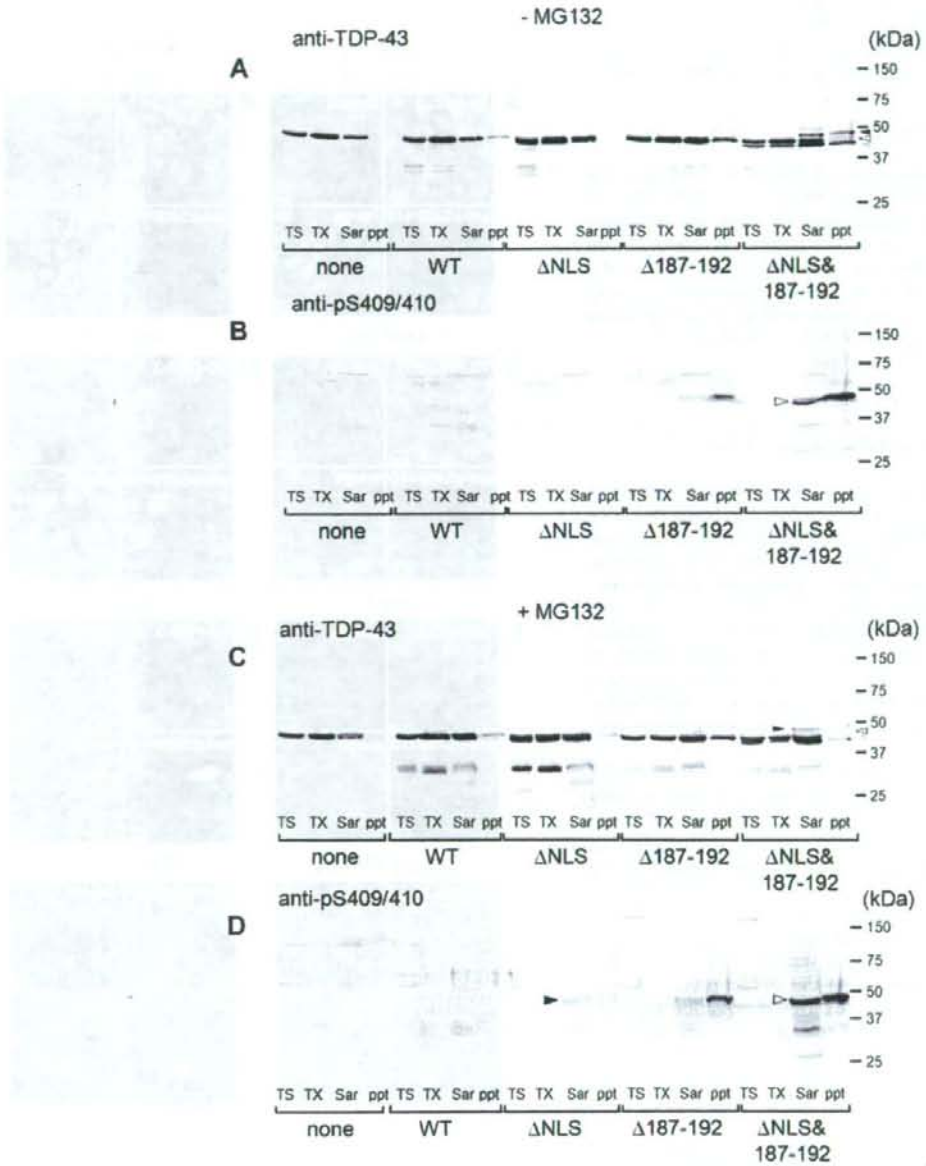

Fig. 4. Immunoblot analyses of intracellular inclusions of deleted TDP-43 mutants in SH-SY5Y cells. Untransfected cells (none) and cells 72 h post transfection with wild-type (WT) or TDP-43 deletion mutants, before (A and B) and after (C and D) treatment with MG132 (1 μM overnight), were sequentially extracted with Tris–saline (TS), 1% Triton-X (TX) and 1% Sarkosyl (Sar), and these supernatants and the Sarkosyl-insoluble pellets (ppt) were run on SDS–PAGE, transferred to PVDF membrane and probed with anti-TDP-43 antibody (A and C) and anti-pS409/410 (B and D).